

POLARIMETRIC RADAR CALIBRATION TECHNIQUES

F.T. Ulaby
M.W. Whitt
K. Sarabandi
P.F. Polatin
V.V. Liepa

Radiation Laboratory
Department of Electrical Engineering
and Computer Science
The University of Michigan
Ann Arbor, MI 48109

July, 1989

PREFACE

This report contains three technical papers concerned with the calibration of polarimetric radar systems. All three papers have been submitted to scientific journals for publication. Because of the strong current interest in this subject, we decided to print and distribute the three papers as a single unit under this report.

The three papers are:

- (1) "Calibration of Polarimetric Radar Systems with Good Polarization Isolation," by K. Sarabandi, F.T. Ulaby, and M.A. Tassoudji
- (2) "A General Polarimetric Radar Calibration Technique: Theory and Experiment. Part I - Theory," by M.W. Whitt and F.T. Ulaby
- (3) "A General Polarimetric Radar Calibration Technique: Theory and Experiment. Part II - Experiment," by F.T. Ulaby, P.F. Polatin, M. Whitt, and V. Liepa.

CALIBRATION OF POLARIMETRIC RADAR SYSTEMS WITH GOOD POLARIZATION ISOLATION

K. Sarabandi
F.T. Ulaby
M.A. Tassoudji

December, 1988

The authors are with the Radiation Laboratory, EECS Department, University of Michigan, Ann Arbor, MI 48109.

This work was supported by NASA Grant NAGW-733 and NASA/JPL contract 957191.

List of Figures

1	Geometry of scattering of a plane wave from a particle.	11
2	Simplified block diagram of a dual polarized radar system.	12
3	Automatic radar cross section measurement setup.	13
4	Geometry of scattering of a plane from a long, thin cylinder.	14
5	Theoretical values for radar cross section versus tilt angle of a cylinder with L=30.48 cm and D=1.625 mm, (—)hh, (- -)vv, (- - -)hv.	15
6	Theoretical values for relative phase (to vv) of the elements of scattering matrix versus tilt angle of a cylinder with L=30.48 cm and D=1.625 mm, (—)hh and (- - -)hv.	16
7	Geometry of a wire-mesh	17
8	Radar cross section (hh) versus frequency of a cylinder with L=30.48 cm and D=1.625 mm, (—)measured and (- - -)theory.	18
9	Radar cross section (vv) versus frequency of a cylinder with L=30.48 cm and D=1.625 mm, (—)measured and (- - -)theory.	19
10	Radar cross section (hv) versus frequency of a cylinder with L=30.48 cm and D=1.625 mm, (—)measured and (- - -)theory.	20
11	Relative phase S_{hh} (to S_{vv}) versus frequency of a cylinder with L=30.48 cm and D=1.625 mm, (—)measured and (- - -)theory.	21
12	Relative phase S_{hv} (to S_{vv}) versus frequency of a cylinder with L=30.48 cm and D=1.625 mm, (—)measured and (- - -)theory.	22

Abstract- A practical technique is proposed for calibrating single-antenna polarimetric radar systems using a metal sphere plus any second target with strong cross-polarized radar cross section. This technique assumes perfect isolation between antenna ports. It is shown that all magnitudes and phases (relative to one of the like-polarized linear polarization configurations) of the radar transfer function can be calibrated without knowledge of the scattering matrix of the second target. Comparison of values measured (using this calibration technique) for a tilted cylinder at X-band with theoretical values shows agreement within ± 0.3 dB in magnitude and $\pm 5^\circ$ in phase. The radar overall cross-polarization isolation was 25 dB. The technique is particularly useful for calibrating a radar under field conditions because it does not require careful alignment of calibration targets.

1 Introduction

A polarimetric radar is a phase-coherent instrument used to measure the polarization scattering matrix \mathbf{S} of point or distributed targets. The matrix \mathbf{S} relates the field \mathbf{E}^s scattered by the target to the field \mathbf{E}^i of a plane wave incident upon the target [1, p.1087],

$$\mathbf{E}^s = \frac{e^{-ikr}}{r} \mathbf{S} \mathbf{E}^i, \quad (1)$$

where r is the distance from the center of the target to the point of observation and k is the wave number. For a plane wave incident upon the particle in the direction $\hat{\mathbf{k}}_i$, its electric field vector may be written in terms of vertical and horizontal polarization components, E_v^i and E_h^i , using the coordinate system $(\hat{\mathbf{v}}_i, \hat{\mathbf{h}}_i, \hat{\mathbf{k}}_i)$ shown in Fig. 1,

$$\mathbf{E}^i = (E_v^i \hat{\mathbf{v}}_i + E_h^i \hat{\mathbf{h}}_i) e^{-ik \hat{\mathbf{k}}_i \cdot \mathbf{r}}, \quad (2)$$

where

$$\hat{\mathbf{v}}_i = \cos\theta_i \cos\phi_i \hat{\mathbf{x}} + \cos\theta_i \sin\phi_i \hat{\mathbf{y}} - \sin\theta_i \hat{\mathbf{z}} \quad (3)$$

$$\hat{\mathbf{h}}_i = -\sin\phi_i \hat{\mathbf{x}} + \cos\phi_i \hat{\mathbf{y}} \quad (4)$$

$$\hat{\mathbf{k}}_i = \sin\theta_i \cos\phi_i \hat{\mathbf{x}} + \sin\theta_i \sin\phi_i \hat{\mathbf{y}} + \sin\theta_i \hat{\mathbf{z}}. \quad (5)$$

In (2), a time dependence of the form $e^{+i\omega t}$ is assumed and suppressed.

The far-field wave scattered in the direction $\hat{\mathbf{k}}_s$ is a spherical wave given by

$$\mathbf{E}^s = E_v^s \hat{\mathbf{v}}_s + E_h^s \hat{\mathbf{h}}_s, \quad (6)$$

where $(\hat{\mathbf{v}}_s, \hat{\mathbf{h}}_s, \hat{\mathbf{k}}_s)$ are defined by the same expressions given in (3) to (5) except for replacing the subscript i with the subscript s . For the backscattering case, $\theta_i + \theta_s = \pi$, $\phi_i + \phi_s = \pi$, $\hat{\mathbf{k}}_s = -\hat{\mathbf{k}}_i$, $\hat{\mathbf{v}}_s = \hat{\mathbf{v}}_i$, and $\hat{\mathbf{h}}_s = -\hat{\mathbf{h}}_i$.

In matrix form, (1) may be rewritten as

$$\begin{bmatrix} E_v^s \\ E_h^s \end{bmatrix} = \frac{e^{-ikr}}{r} \begin{bmatrix} S_{vv} & S_{vh} \\ S_{hv} & S_{hh} \end{bmatrix} \begin{bmatrix} E_v^i \\ E_h^i \end{bmatrix} \quad (7)$$

where

$$\mathbf{S} = \begin{bmatrix} S_{vv} & S_{vh} \\ S_{hv} & S_{hh} \end{bmatrix} \quad (8)$$

is defined in terms of the scattering amplitudes S_{mn} with m and n denoting the polarization (v or h) of the scattered and incident fields, respectively. The scattering amplitude S_{mn} is, in general, a complex quantity comprised of a magnitude $s_{mn} = |S_{mn}|$ and a phase angle ψ_{mn} ,

$$S_{mn} = s_{mn} e^{i\psi_{mn}}; \quad m, n = v \text{ or } h, \quad (9)$$

and it is related to the radar cross section (RCS) of the target, σ_{mn} , by

$$\begin{aligned} \sigma_{mn} &= 4\pi |S_{mn}|^2 \\ &= 4\pi s_{mn}^2; \quad m, n = v \text{ or } h. \end{aligned} \quad (10)$$

Interest in measuring \mathbf{S} stems from the fact that if the elements of \mathbf{S} are known, we can compute the RCS of the target that would be observed by a radar with any specified combination of transmit and receive antenna configuration, including elliptical and circular polarizations [2]. In fact, we do not need to know all four magnitudes and four phases of \mathbf{S} in order to synthesize the desired RCS; it is sufficient to know the four magnitudes and any three of the phase angles,

measured with respect to the fourth as reference. Thus, if we choose ψ_{vv} as reference, we can write (8) in the form

$$\begin{aligned} \mathbf{S} &= e^{i\psi_{vv}} \begin{bmatrix} s_{vv} & s_{vh} e^{i\psi'_{vh}} \\ s_{hv} e^{i\psi'_{hv}} & s_{hh} e^{i\psi'_{hh}} \end{bmatrix} \\ &= e^{i\psi_{vv}} \mathbf{S}' \end{aligned} \quad (11)$$

where

$$\psi'_{mn} = \psi_{mn} - \psi_{vv}, \quad m,n=v \text{ or } h. \quad (12)$$

For backscattering, the reciprocity theorem mandates that $S_{hv} = S_{vh}$, which further reduces the number of unknown quantities from 7 to 5.

The formulation given above is equally applicable to a distributed target. If the effective area illuminated by the radar antenna is A , the polarimetric scattering behavior of the distributed target is characterized by the differential scattering matrix $\mathbf{S}^0 = \mathbf{S}/\sqrt{A}$.

In principle, S_{vv} and S_{hv} can be determined by measuring E_v^s and E_h^s with the target illuminated by a pure vertically polarized wave $\mathbf{E}^i = E_v^i \hat{\mathbf{v}}_i$ and, similarly, S_{vh} and S_{hh} can be determined by measuring the same quantities when the target is illuminated by $\mathbf{E}^i = E_h^i \hat{\mathbf{h}}_i$. Such a procedure requires that (1) the transmit and receive antennas of the measurement system each have excellent isolation between its v- and h-ports, and (2) the receive-transmit transfer functions of the measurement system be known for all four polarization combinations (vv, vh, hv, and hh). Design techniques are currently available to achieve antenna polarization isolation on the order of 30 dB. For a radar scatterometer system intended to measure the differential scattering matrices of distributed targets such as ground surfaces and vegetation canopies, such a level of isolation is sufficient to insure good measurement accuracy of the magnitudes and phases of all four scattering amplitudes. The error associated with measuring the like-polarized components S_{vv} and S_{hh} is negligibly small, and for S_{hv} (and S_{vh}) the error also is less than 0.85 dB if $|S_{hv}| / |S_{vv}| \geq 0.31$, which corresponds to $\sigma_{hv}/\sigma_{vv} \geq 0.1$ (or -10 dB). For natural targets the like- and cross-polarized components, S_{hv} and S_{vv} for example, are uncorrelated and for $\sigma_{hv}/\sigma_{vv} \geq 0.01$ the associated error would be less than 0.4 dB.

If the radar antennas do not individually have good polarization isolation between their v- and h-ports, it is necessary to characterize each antenna by a polarization distortion matrix that accounts for the coupling between the two ports, and to use at least two, and preferably three, targets of known scattering matrices in order to calibrate the radar completely [3]. This case is outside the scope of this paper and will be the subject of future papers. Instead, we will now focus our attention on the problems associated with measuring the receiver-transmitter transfer function for a radar with reasonably good overall cross-polarization isolation using suitable external calibration targets.

2 SYSTEM TRANSFER FUNCTION

Although a radar may use a single antenna to provide both transmit and receive functions and may also use a polarization switching network capable of exciting either v- or h-polarized waves in the antenna, we shall use the block diagram shown in Fig. 2 to represent the general case of a two-pole transmitter and a two-pole receiver. Assuming perfect isolation between antenna ports, the voltage received by the v-polarized receive antenna due to illumination of a target at range r by a v-polarized wave is given by

$$\begin{aligned} E_{vv} &= \left[\frac{P_t G_t G_r \lambda^2}{(4\pi)^2 r^4} \right]^{1/2} e^{-i2kr} R_v T_v \sqrt{4\pi} S_{vv} \\ &= \frac{K}{r^2} e^{-i2kr} R_v T_v S_{vv} \end{aligned} \quad (13)$$

where

$$K = \left[\frac{P_t G_t G_r \lambda^2}{(4\pi)^2} \right]^{1/2}, \quad (14)$$

S_{vv} is the scattering amplitude of the target, P_t is the transmitted power, and G_r and G_t are the nominal gains of the transmit and receive antennas. The quantities R_v and T_v are field transfer function for the receive and transmit antennas, respectively, which account for the deviation in both amplitude and phase from the nominal condition described by $G_t G_r$. Similarly, for any receive-transmit polarization configuration, we have

$$E_{mn} = \frac{K}{r^2} e^{-i2kr} R_m T_n S_{mn}, \quad m, n = v \text{ or } h. \quad (15)$$

3 CALIBRATION

The standard calibration approach involves the use of one reference target of known scattering matrix. Upon measuring E_{mn} with S_{mn} known, the quantity $(KR_m T_n)$ can be determined in amplitude and phase, with the latter being relative to some reference distance time delay.

In principle, the procedure is simple and straightforward. The problem arises when we need to select a reference target of known scattering matrix. The metal sphere is the easiest target to align and its scattering matrix can be computed exactly [4, p.297]. Unfortunately, it can only be used to calibrate the vv- and hh-channels because its $S_{hv}^{sp} = S_{vh}^{sp} = 0$. Targets that exhibit significant cross-polarized scattering include the dihedral corner reflector, tilted cylinders, and others, but scattering from such targets is inherently sensitive to the orientation of the target relative to the $(\hat{v}_i, \hat{h}_i, \hat{k}_i)$ coordinate system. This, and other factors such as edge scattering, may lead to significant errors between the calculated values of the scattering amplitudes and their actual values. The orientation problem may be reduced down to an acceptable level when operating in an anechoic chamber under controlled laboratory conditions, but it poses a difficult problem when it is necessary to calibrate a truck-mounted scatterometer, for example, under field conditions.

To solve this problem, we propose to use two reference targets, namely a sphere and any target with strong cross-polarized RCS. As will be shown below, it is not necessary to know the RCS of the second reference target in order to calibrate the radar system.

First, let us use a metal sphere of known size, and place it at a distance r_0 from the radar. The scattering amplitudes of a metal sphere are $S_{hh} = S_{vv} \equiv S_0$, and $S_{hv} = S_{vh} = 0$. The received fields for vv and hh polarizations are

$$E_{vv}^0 = \frac{K}{r_0^2} e^{-i2kr_0} R_v T_v S_0 \quad (16)$$

$$E_{hh}^0 = \frac{K}{r_0^2} e^{-i2kr_0} R_h T_h S_0 \quad (17)$$

where the subscript and superscript 0 denote quantities associated with the metal sphere. For a test target with unknown scattering matrix S^u , placed at a distance r_u from the radar, the

received field is

$$E_{vv}^u = \frac{K}{r_u^2} e^{-i2kr_*} R_v T_v S_{vv}^u, \quad (18)$$

$$E_{hv}^u = \frac{K}{r_u^2} e^{-i2kr_*} R_h T_v S_{hv}^u, \quad (19)$$

$$E_{hh}^u = \frac{K}{r_u^2} e^{-i2kr_*} R_h T_h S_{hh}^u, \quad (20)$$

$$E_{vh}^u = \frac{K}{r_u^2} e^{-i2kr_*} R_v T_h S_{vh}^u. \quad (21)$$

From (16) and (18), and similarly from (17) and (20), we obtain the following expressions for the unknown like-polarized scattering amplitudes

$$S_{vv}^u = \left(\frac{E_{vv}^u}{E_{vv}^0} \right) \left(\frac{r_u}{r_0} \right)^2 e^{-i2k(r_0 - r_*)} S_0, \quad (22)$$

$$S_{hh}^u = \left(\frac{E_{hh}^u}{E_{hh}^0} \right) \left(\frac{r_u}{r_0} \right)^2 e^{-i2k(r_0 - r_*)} S_0. \quad (23)$$

All the quantities on the right-hand side of the above two expressions can be measured directly except for S_0 which can be computed precisely using the standard Mie expressions. Small errors in the measurements of the ranges r_u and r_0 will have a minor effect on the magnitude of S_{hh}^u , but may cause a large error in the measurement of the phase angle of S_{hh}^u if the error $\Delta(r_0 - r_*)$ is comparable to λ . However, the phase ψ'_{hh} of S_{hh}^u relative to that of S_{vv}^u is independent of $(r_0 - r_*)$.

Next, let us use any point target that exhibits strong cross-polarized scattering, and let us measure the received field for hv and vh polarizations,

$$E_{hv}^c = \frac{K}{r_c^2} e^{-i2kr_c} R_h T_v S_{hv}^c \quad (24)$$

$$E_{vh}^c = \frac{K}{r_c^2} e^{-i2kr_c} R_v T_h S_{vh}^c \quad (25)$$

where the subscript and the superscript c refers to the cross-polarization calibration target. The reciprocity theorem states that in the backscattering direction, the cross-polarized scattering amplitudes are always equal. Hence,

$$S_{hv}^c = S_{vh}^c \quad (26)$$

and consequently

$$K_1 \equiv \frac{E_{hv}^c}{E_{vh}^c} = \frac{R_h T_v}{R_v T_h} \quad (27)$$

If we define the additional quantity K_2 as

$$\begin{aligned} K_2 &= E_{vv}^0 E_{hh}^0 \\ &= \frac{K^2}{r_0^4} e^{-i4kr_0} R_v T_v R_h T_h S_0^2, \end{aligned} \quad (28)$$

and use it in combination with (19), (21), and (27), we can obtain the following expressions for the cross-polarized scattering amplitudes of the test target:

$$S_{hv}^u = \frac{E_{hv}^u}{\sqrt{K_1 K_2}} \left(\frac{r_u}{r_0} \right)^2 e^{-i2k(r_0 - r_u)} S_0 \quad (29)$$

$$S_{vh}^u = \sqrt{\frac{K_1}{K_2}} E_{vh}^u \left(\frac{r_u}{r_0} \right)^2 e^{-i2k(r_0 - r_u)} S_0 \quad (30)$$

Equations (22), (23), (29), and (30) provide expressions for the four scattering amplitudes in terms of (1) the like-polarized received voltages for the metal sphere, E_{vv}^0 and E_{hh}^0 , (2) the ratio of the cross-polarized received voltages for the second calibration target, $K_1 = E_{hv}^c/E_{vh}^c$, (3) the like-polarized scattering amplitude of the sphere, S_0 , and (4) the ranges to the sphere and the test target, r_0 and r_u . Note that knowledge of the scattering amplitude of the second calibration target is not required.

4 COMPARISON WITH MEASURED DATA

To verify the validity of the proposed calibration technique summarized by equations (22), (23), (29), and (30), we measured the scattering matrix of a tilted cylinder with an X-band radar. The radar is an HP 8753-based dual polarized scatterometer operating in continuous chirped mode (9-10 GHz). The antenna of the scatterometer is a square horn with an orthogonal mode transducer (OMT). The overall cross-polarization isolation of the system is better than 25 dB. The scattering measurements were performed in a 13-m long anechoic chamber using the setup diagrammed in Fig. 3. A similar system with an operating frequency of 35 GHz is described in [5].

Although an exact theoretical solution for a finite-length, conducting cylinder does not exist, the solution based on the assumption that the current along the axis of the cylinder is constant provides accurate results in the specular direction, if the length of the cylinder (L) is much larger than the wavelength [6]. In order to minimize edge effects caused by scattering by the ends of the cylinder, the diameter of the cylinder (D) must also be chosen to be much smaller than the wavelength. Hence, we selected a cylinder with $L=30.48$ cm and $D=1.625$ mm.

Correct positioning of the test target with respect to the antenna coordinates is very important. First, the target must be placed at the center of the antenna beam in order to avoid phase variations of the incident field along the axis of the target. This was accomplished using a pair of two laser beams. Another alignment parameter that has to be carefully controlled is the angle ϕ between the incidence direction ($\hat{\mathbf{k}}_i$) and the projection of the cylinder axis onto the horizontal plane (Fig. 4). The elements of the scattering matrix are very sensitive to variations in azimuth angle and the rate of change is proportional to the length of the cylinder. This angle was set to 90° with a fine-control stepper motor (steps of a fraction of a tenth of a degree) by maximizing the received power. The third alignment parameter is the tilt angle θ which is the angle between the axis of the cylinder and the vertical direction ($\hat{\mathbf{v}}_i$). Accurate setting of this angle is very difficult. The sensitivity due to misalignment in θ is shown in Fig. 5 for amplitude and in Fig. 6 for relative phase (to vv) of the elements of the scattering matrix using theoretical expressions [6]. This angle was set to 50° using an inclinometer.

Under the mentioned conditions a signal to noise ratio of 25 dB was achieved for the test cylinder and after background subtraction the signal to noise ratio was improved to 40 dB. To eliminate short-range reflections from the antenna circulators, the returned signal was time-gated, as a result of which the frequency response around the beginning and the end of the frequency band was distorted and discarded.

A 15-cm sphere was used for sphere calibration and a 45° wire-mesh (Fig. 7) was employed as the cross-polarization target. The distances of all the targets from the scatterometer, which were accurately measured using the time-domain feature of the HP 8753 Vector Network Analyzer,

were arranged such that $r_0 = r_c = r_u$. The measured amplitudes of the scattering matrix elements of the cylinder are compared with theoretical values in Figures 8-10. The measured values are within $\pm 0.3dB$ of the theoretical results. For relative phase, the measured values (Figs. 11 and 12) are within $\pm 5^\circ$ of theoretical predictions. These deviations are attributed to alignment errors and to the imperfect polarization isolation of the antenna.

5 CONCLUSIONS

The excellent agreement between measurements and theory demonstrates that the calibration technique proposed in this paper is an effective approach for calibrating single-antenna polarimetric radar systems. The technique is particularly useful for field operations because it does not require accurate alignment of calibration targets or knowledge of the radar cross section of the depolarization target.

Acknowledgements: The authors wish to acknowledge the assistance of Mr. Martin Kuttner, Dr. Valdis Liepa and Mr. Paul Polatin.

REFERENCES

- [1] Ulaby, F.T., R.K. Moore, and A.D. Fung, Microwave Remote Sensing: Active and Passive, Vol. III, Dedham, MA: Artech House, Inc., 1986.
- [2] Zebker, H.A., J.J. van Zyl, and D.n. Held, "Imaging Radar Polarimetry from Wave Synthesis," *J. Geophys. Res.*, Vol. 92, No. 81, January 1987, pp. 683-701.
- [3] Barnes, R.M., "Polarimetric Calibration Using In-scene Reflectors," MIT Lincoln Lab Technical Report TT-65, September 1986.
- [4] Ulaby, F.T., R.K. Moore, and A.D. Fung, Microwave Remote Sensing: Active and Passive, Vol. I, Reading, MA: Addison Wesley, 1981.
- [5] Whitt, M.W., F.T. Ulaby, "Millimeter-Wave Polarimetric Measurements of Artificial and Natural Targets," *IEEE Transactions on Geoscience and Remote Sensing*, Vol. GE-26, No. 5, September 1988, pp. 562-573.
- [6] Ruck, G.T., D.E. Barrick, W.D. Stuart, and C.K. Krichbaum, Radar Cross Section Handbook, Vol. 1, New York, NY: Plenum Press, 1970.

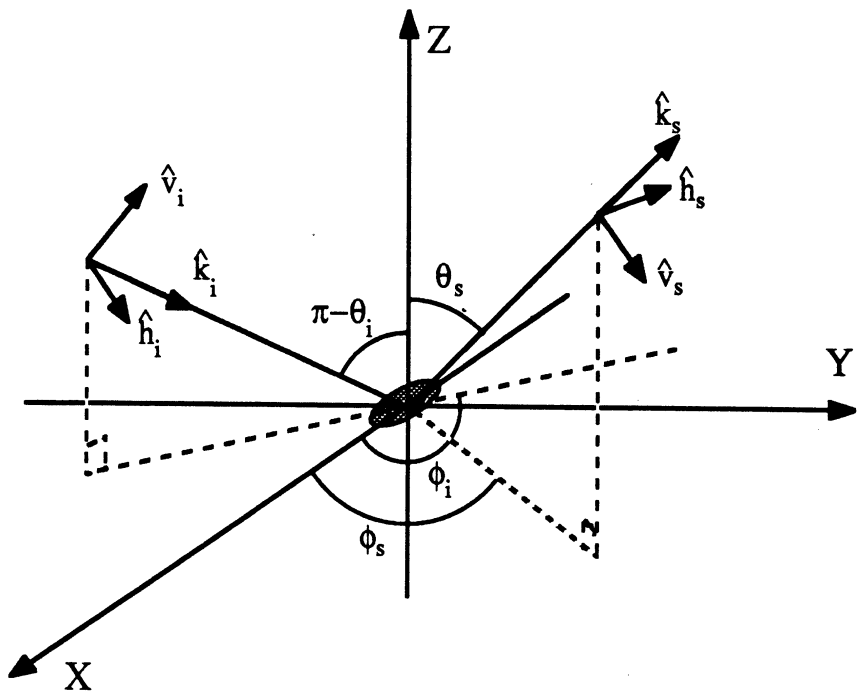


Figure 1: Geometry of scattering of a plane wave from a particle.

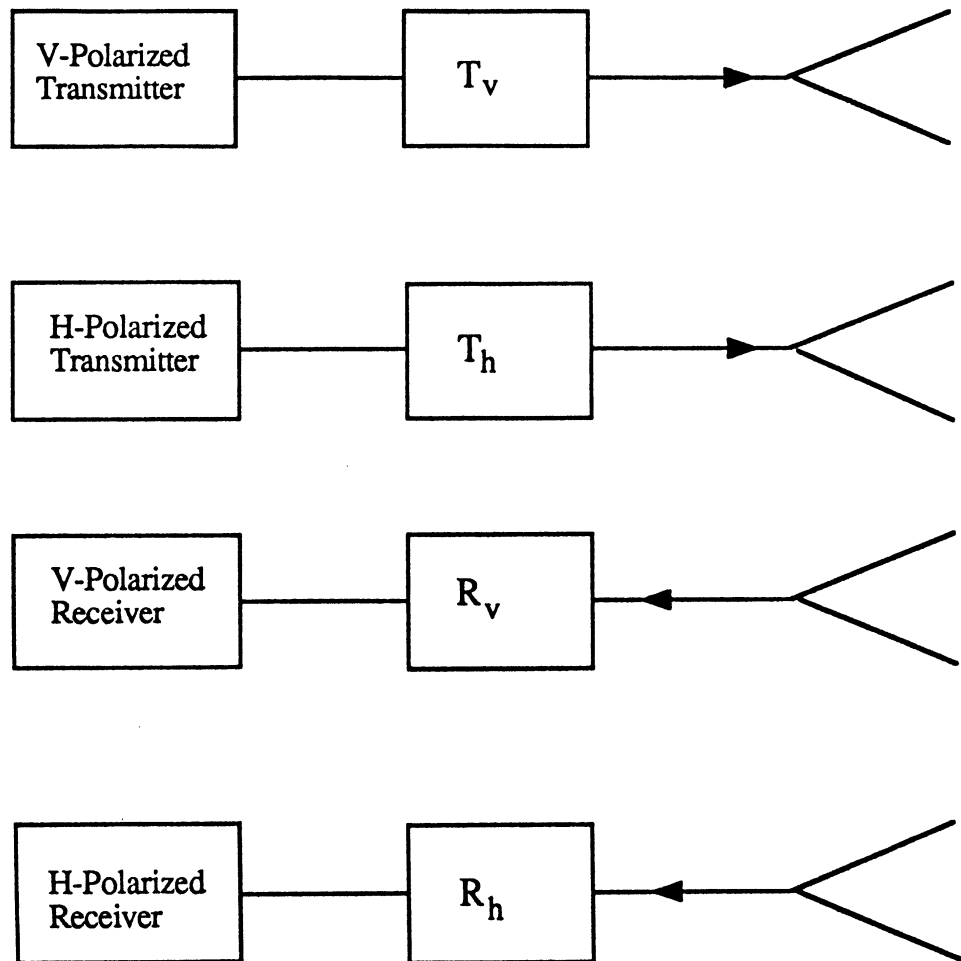


Figure 2: Simplified block diagram of a dual polarized radar system.

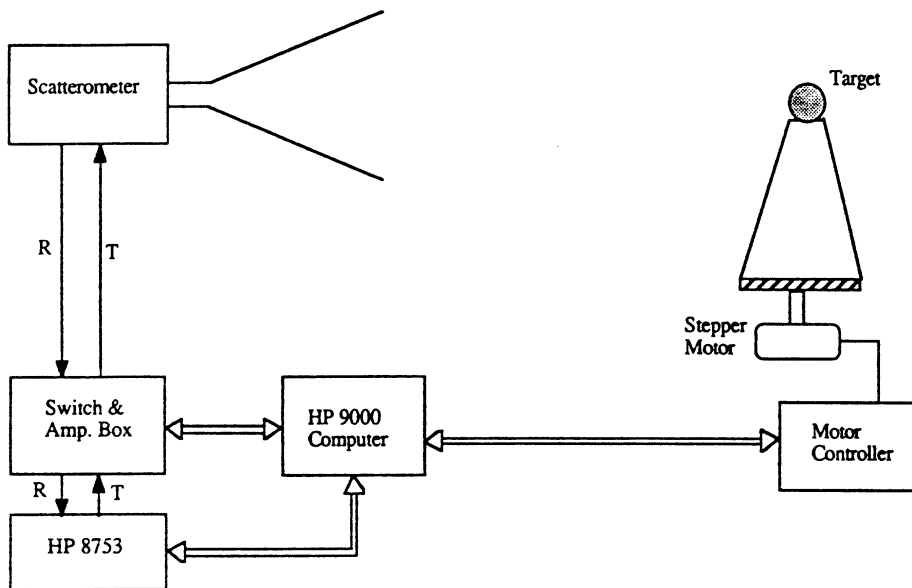


Figure 3: Automatic radar cross section measurement setup.

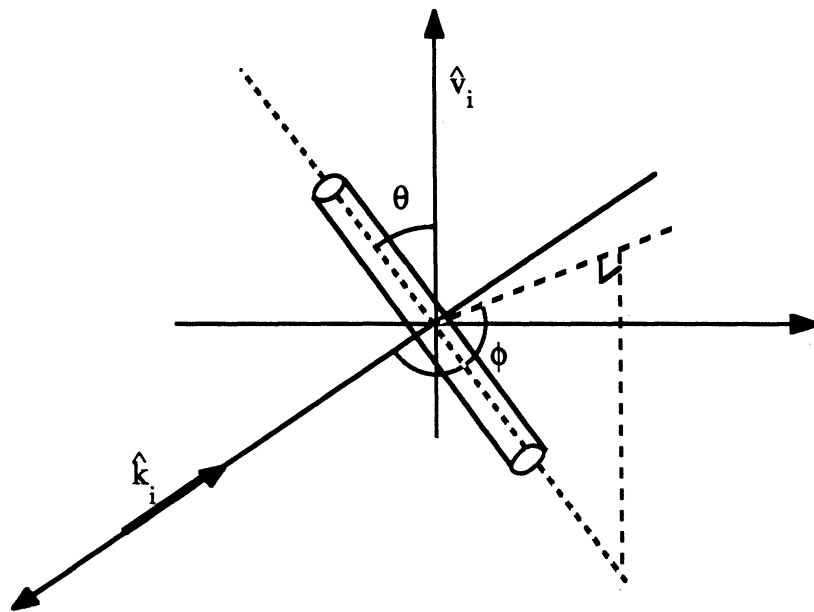


Figure 4: Geometry of scattering of a plane from a long, thin cylinder.

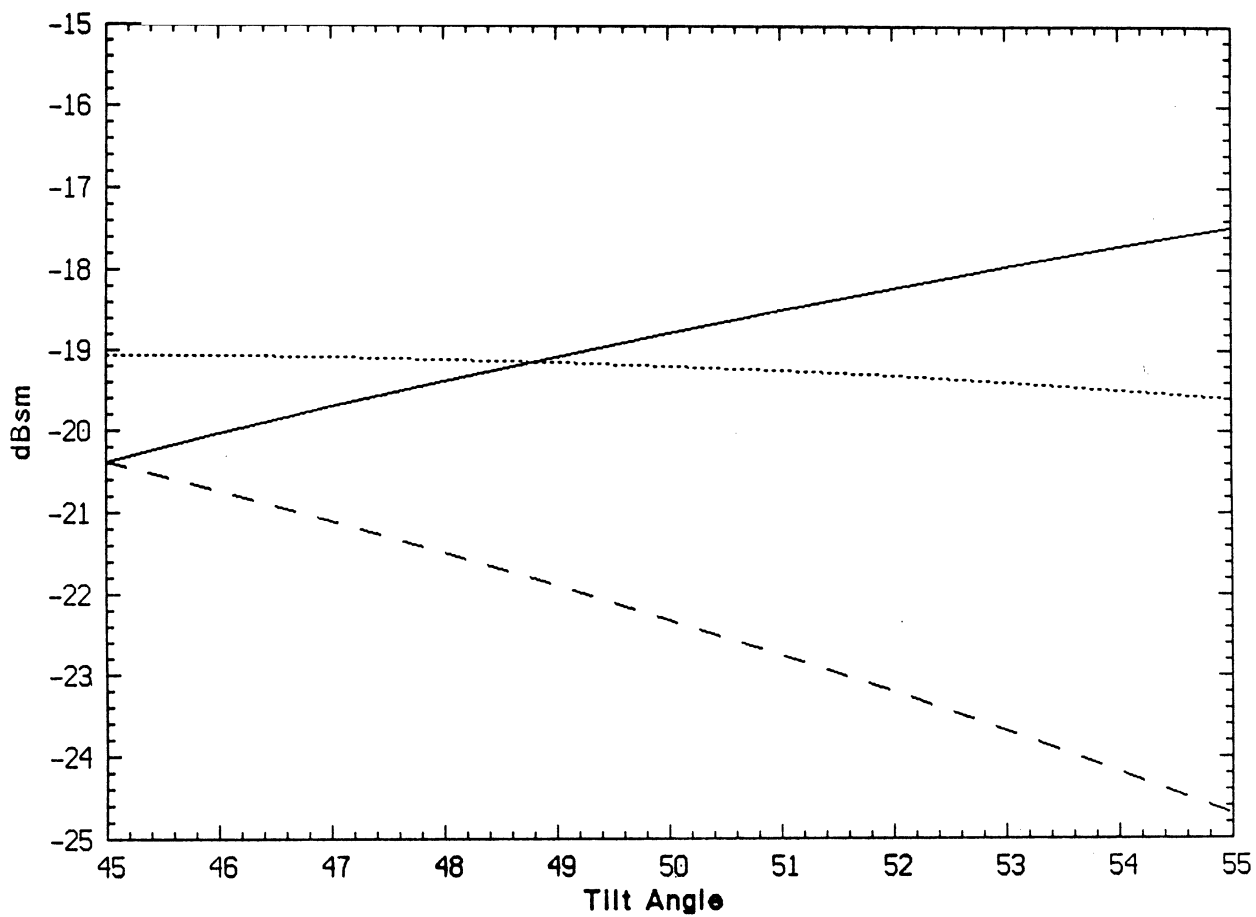


Figure 5: Theoretical values for radar cross section versus tilt angle of a cylinder with $L=30.48$ cm and $D=1.625$ mm, (—)hh, (- -)vv, (- - -)hv.

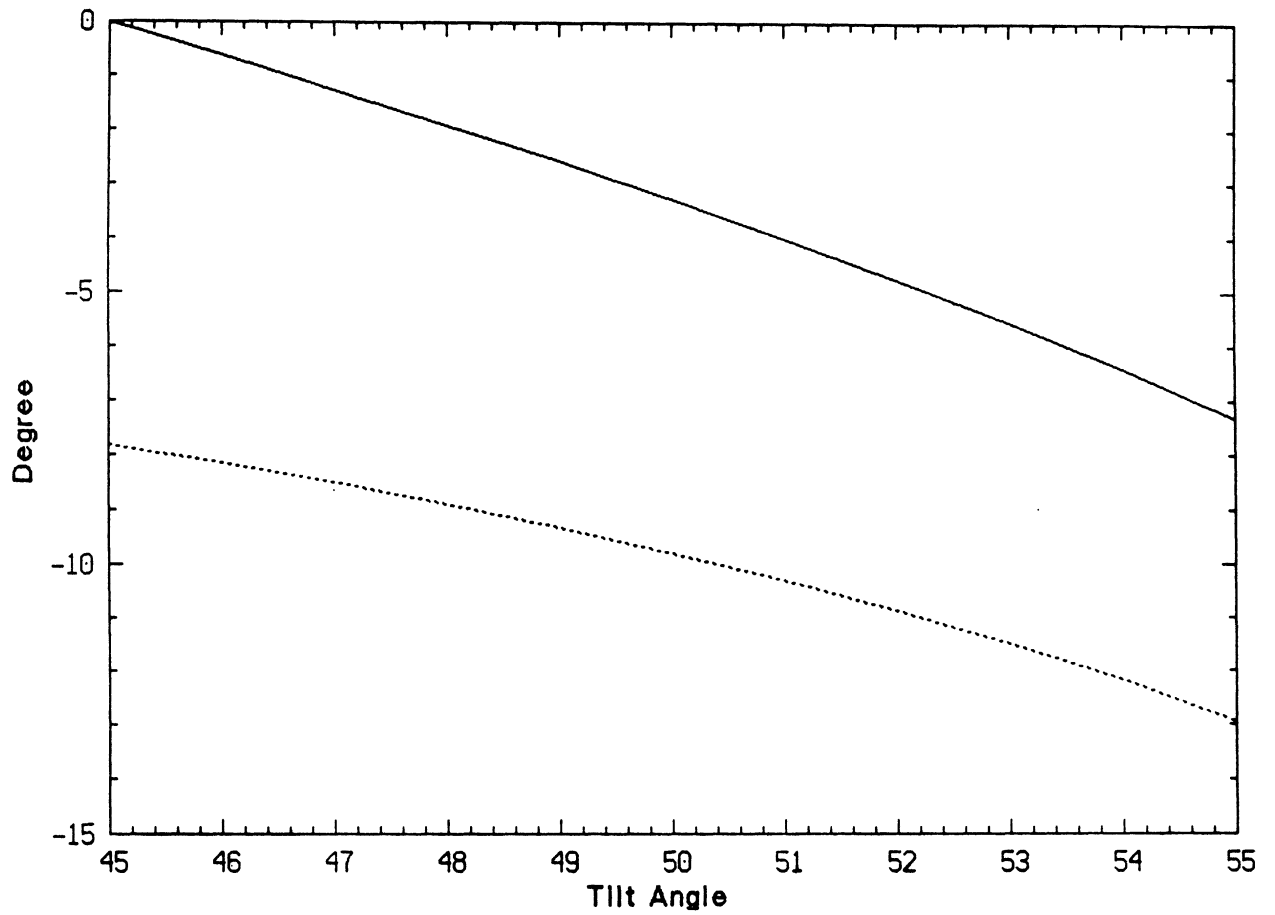


Figure 6: Theoretical values for relative phase (to vv) of the elements of scattering matrix versus tilt angle of a cylinder with $L=30.48$ cm and $D=1.625$ mm, (—)hh and (- - -)hv.

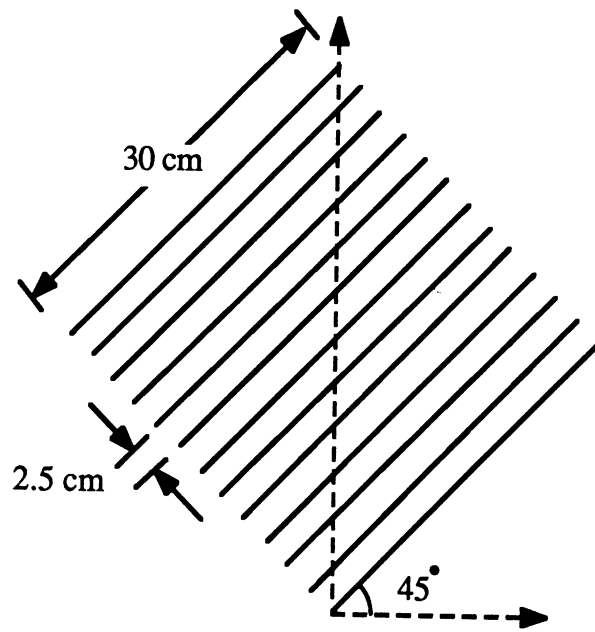


Figure 7: Geometry of a wire-mesh

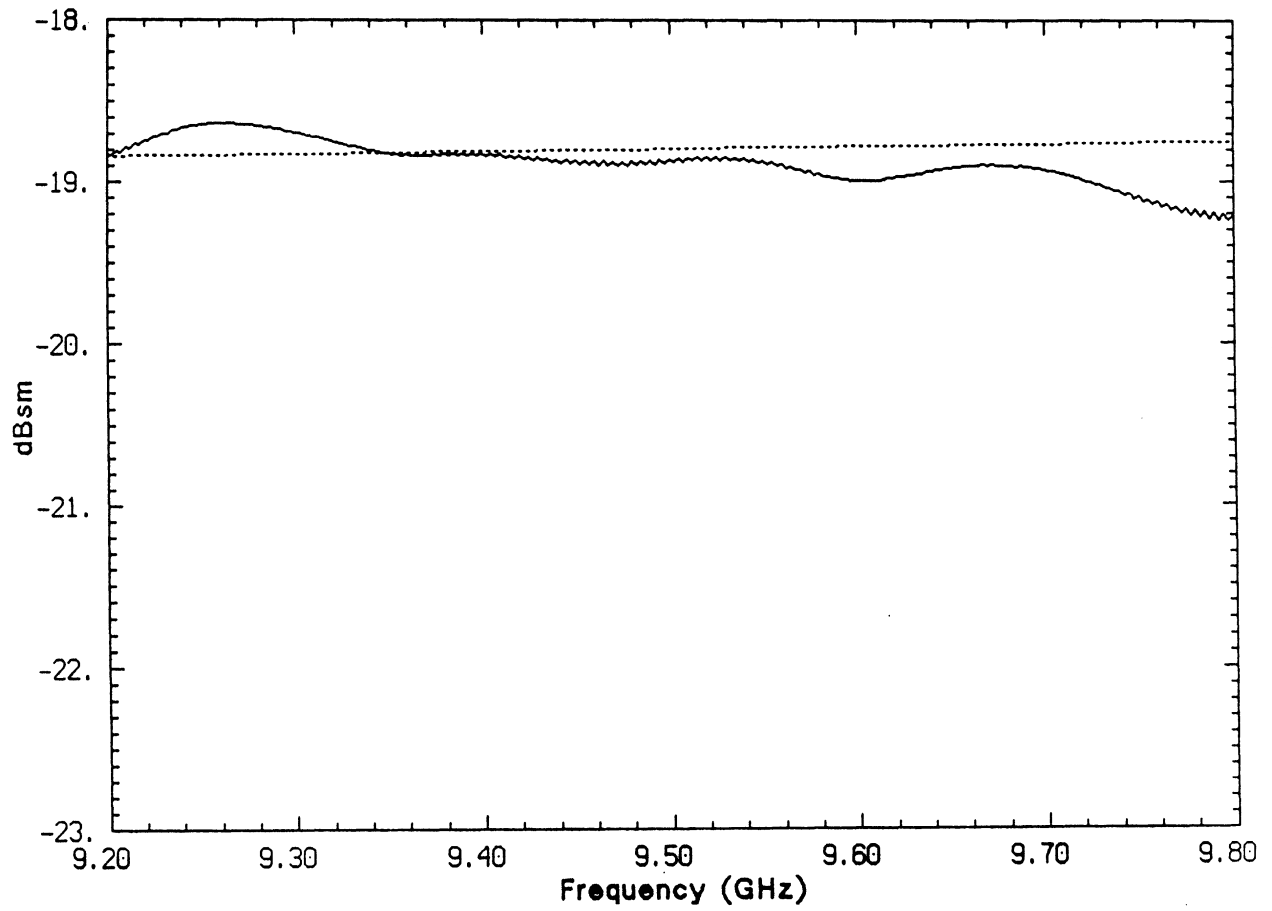


Figure 8: Radar cross section (hh) versus frequency of a cylinder with $L=30.48$ cm and $D=1.625$ mm, (—)measured and (- - -)theory.

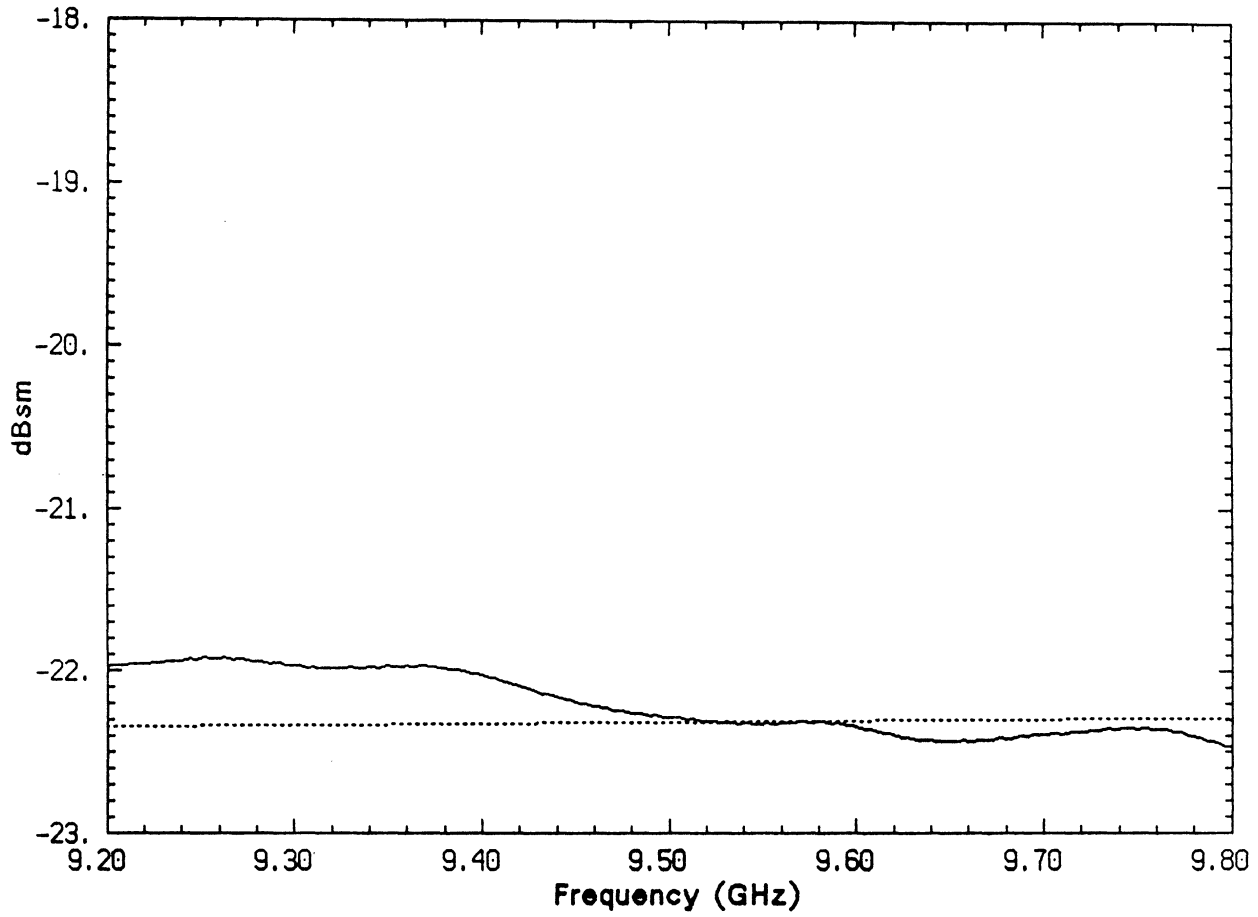


Figure 9: Radar cross section (vv) versus frequency of a cylinder with $L=30.48$ cm and $D=1.625$ mm, (—)measured and (- -)theory.

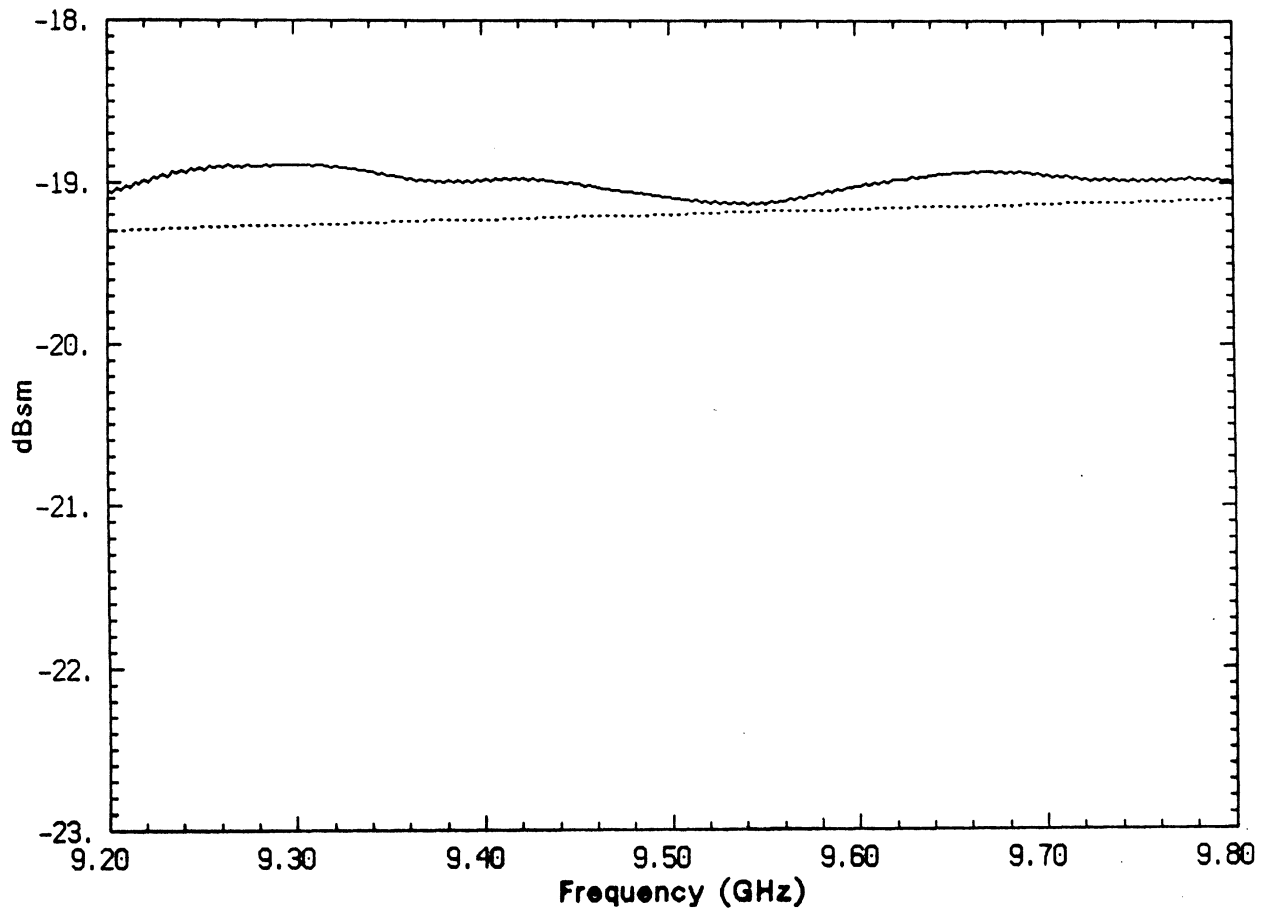


Figure 10: Radar cross section (hv) versus frequency of a cylinder with $L=30.48$ cm and $D=1.625$ mm, (—)measured and (- - -)theory.

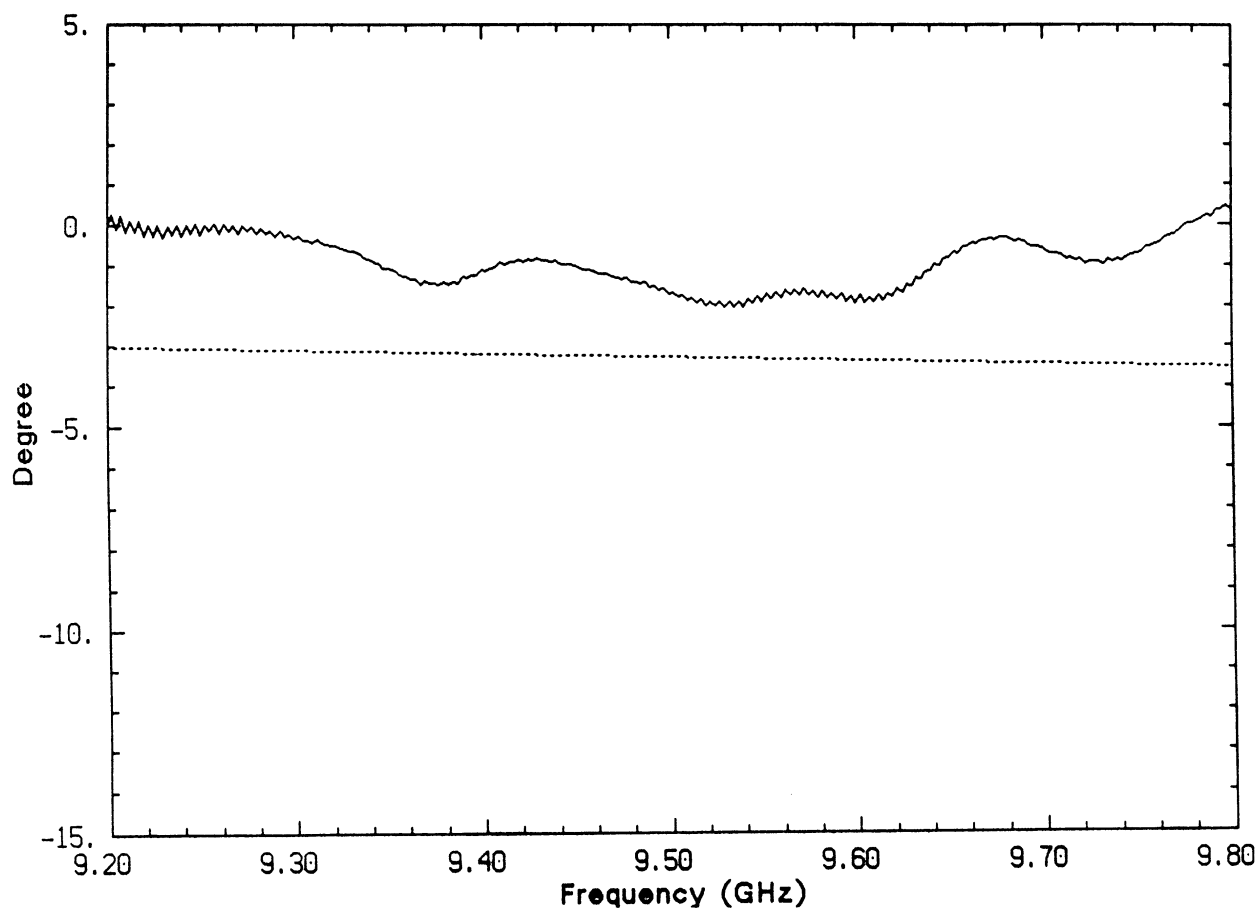


Figure 11: Relative phase S_{hh} (to S_{vv}) versus frequency of a cylinder with $L=30.48$ cm and $D=1.625$ mm, (—)measured and (- - -)theory.

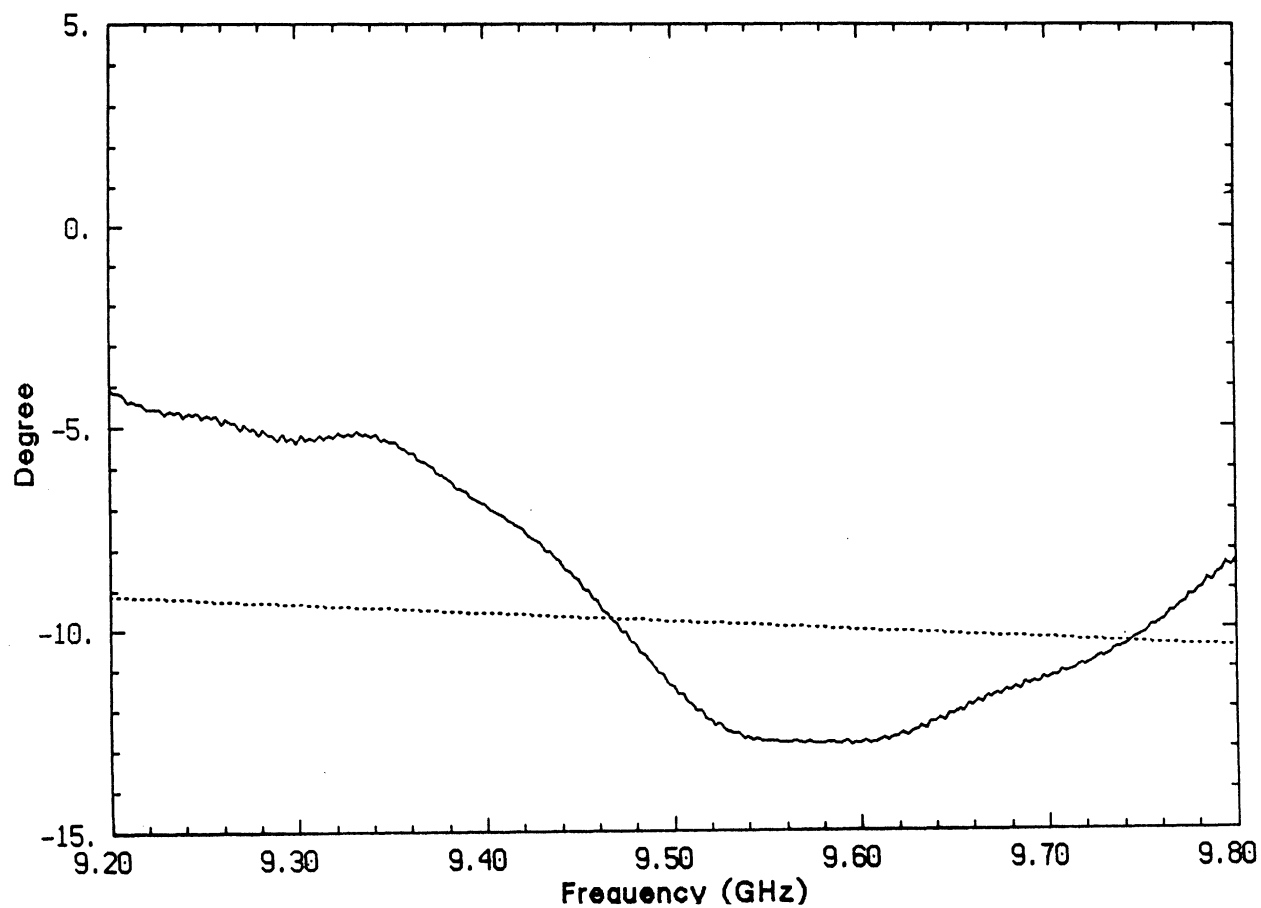


Figure 12: Relative phase S_{hv} (to S_{vv}) versus frequency of a cylinder with $L=30.48$ cm and $D=1.625$ mm, (—)measured and (- - -)theory.

A GENERAL POLARIMETRIC RADAR CALIBRATION
TECHNIQUE: THEORY AND EXPERIMENT

PART I – THEORY

M.W. Whitt

F.T. Ulaby

July 31, 1989

Radiation Laboratory
Department of Electrical Engineering
and Computer Science
The University of Michigan
Ann Arbor, MI 48109-2122

Abstract

A polarimetric calibration procedure useful for both laboratory and field measurements is introduced. The procedure requires measurements of three known targets in order to determine the distortion matrices that characterize the effect of the measurement system on the transmitted and received waves. The scattering matrices for the known targets can be of any form, providing that a limited set of constraints are satisfied. The approach involves forming matrix products from the measured scattering matrices to obtain a similarity transformation where the transformation matrix is the unknown distortion matrix. The relationships between the eigenvalues and eigenvectors of the similar matrices are then used to solve for the distortion matrices. A special case, wherein the transmit and receive distortion matrices are the transpose of one another, is considered also. This form can be used with some single antenna systems, and it has the advantage that only two known targets need to be measured. Constraints on the scattering matrices for the two known targets are given for this case also. Finally, application of the technique to measuring the propagation characteristics of random media is briefly discussed.

1 Introduction

A Traditional radar system transmits and receives a single polarization. Hence, the scattering characteristics of the illuminated scene are obtained for only one transmit and receive polarization combination. Because the radar measures only the amplitude of the scattered wave, any information contained in the phase or polarization of the wave is lost. However, a polarimetric radar system measures the complete scattering matrix (amplitude and relative phase) of the illuminated scene using an orthogonal set of polarization configurations, and this information can be used to synthesize the scattering characteristics of the scene at any arbitrary transmit and receive polarization combination [1,2]. Much of the early research in polarimetry concentrated on point targets, and an extensive review of this history is given by Guili [3]. Polarimetric radars and techniques have received increased attention in the last few years, following the development of several polarimetric imaging radar systems [1,4,5]. Laboratory and truck-based polarimetric radars have also been developed with the advent of the HP 8510 vector network analyzer [6,7,8,11]. With an increasing number of operating polarimetric radars, it has become important to develop effective techniques for accurate polarimetric calibration.

Calibration of polarimetric radar systems has been considered by several investigators in recent years. A technique proposed by Barnes [9] characterizes the errors introduced by the transmitter and receiver in terms of distortion matrices that alter the measured scattering matrix of the target. This calibration tech-

nique requires the measurement of three known targets, some of which have zero elements in their scattering matrices. Two algorithms are proposed by Barnes, differing only in the type of known targets to be measured. A technique similar to the one by Barnes was used by Freeman, et al. [10] where the known target scattering matrices were realized by Polarimetric Active Radar Calibrators (PARC's). A technique introduced by Riegger, et al. [11] characterizes the system errors in terms of coupling coefficients between elements of the theoretical scattering matrix and elements of the measured scattering matrix. It is in essence the same model as used by Barnes, except that Riegger has expanded the matrix product which resulted in twice the number of unknowns. In its most general form, this technique would require the measurement of four known targets to solve for sixteen unknown coupling coefficients. However, Riegger neglects four of the coupling coefficients and reduces the required number of known targets to three.

The calibration techniques described above have a number of disadvantages. The algorithms used by Barnes and Freeman depend upon the actual known targets that are measured. If a new set of targets is used, the derivation must be repeated. In addition, if the scattering matrices of at least some of the targets do not contain zeros, it becomes difficult (if not impossible) to solve for the elements of the distortion matrices. In many cases, the scattering matrix elements are known to be non-zero, but one must assume they are zero for derivation of the calibration algorithms. Relying on certain elements of the scattering matrix to be zero places a considerable restriction on the targets that can be used. This

is seen as a major disadvantage, because one would like to examine a variety of known targets and choose the best possible set. The technique used by Riegger, as already mentioned, introduces more unknowns than required and is therefore inefficient.

Two additional polarimetric calibration techniques are of interest because they require only a single non-depolarizing target (such as a sphere or trihedral) to correct for co-polarized channel imbalance and absolute magnitude errors. The cross-polarization coupling (or cross-talk) errors are corrected using unknown targets. The first technique, proposed by Sarabandi, et al. [12] achieves calibration of the cross-talk errors by measuring any arbitrary depolarizing target. Knowledge of the scattering matrix of the arbitrary target is not required. A similar technique by van Zyl [13] uses measurements of distributed natural targets to determine the cross-talk errors. The advantage of these techniques is their insensitivity to target positioning, which makes them particularly useful in field calibration. The disadvantages, however, include (1) the radar systems are assumed to be reciprocal (i.e., the distortion matrix for reception is the transpose of that for transmission), (2) the cross-talk errors are assumed to be small (i.e., cross-pol isolation is good), and (3) in the case of the technique by van Zyl, the co-polarized and cross-polarized scattering matrix elements from natural distributed targets are assumed to be uncorrelated.

This paper is the first of a set of two papers where we present a general polarimetric calibration technique that is independent of the scattering matrices of the

known targets to be measured. In this paper, we develop the theory and provide an algorithm to be used in the calibration procedure. The second paper [14] uses this algorithm to calibrate an actual radar system, and then compares the results to those of currently available calibration techniques.

The algorithm is obtained by modeling the errors as distortion matrices (see Section 2) in the same way as was done by Barnes [9]. However, no assumptions are made about the form of the distortion matrices. Instead of solving a set of possibly nonlinear equations for the elements of the distortion matrices, an eigenvalue approach is employed. Two types of polarimetric radar systems will be considered: (1) dual antenna systems for which the distortion matrices for transmit and receive are unrelated and (2) specialized single antenna systems for which the distortion is reciprocal. The first type is considered in Section 3, and the second type is considered in Section 4. Finally, we consider application of the technique to measuring the propagation characteristics of random media in Section 5.

2 Distortion Model

When using an ideal polarimetric radar, the measured scattering matrix M of a point target would be equal to its theoretical (or actual) scattering matrix P . Because this is rarely the case, the errors introduced by the radar system must be determined and then the process must be inverted in order to obtain an estimate of the actual scattering matrix. In the present work, we consider two types of errors: additive errors due to the presence of some unknown background and multiplicative

errors which modify the polarization, amplitude, and phase of the transmitted and received waves. The multiplicative errors occur because of unknown gain and phase differences between the vertical and horizontal channels of the system. In order to account for these errors, we write the measured scattering matrix \mathbf{M} for some point target \mathbf{P} as

$$\mathbf{M} = \mathbf{B} + e^{j\phi} r_{vv} t_{vv} \mathbf{R} \mathbf{P} \mathbf{T}, \quad (1)$$

where the matrix \mathbf{B} represents the effect of the background, and the distortion matrices \mathbf{T} and \mathbf{R} represent the effect of the antenna system (or the multiplicative errors) for transmit and receive, respectively. Throughout the paper, all matrices will be considered in the linear (vertical and horizontal) polarization basis; therefore the matrices of equation (1) are represented by

$$\mathbf{M} = \begin{bmatrix} m_{vv} & m_{vh} \\ m_{hv} & m_{hh} \end{bmatrix}, \quad \mathbf{B} = \begin{bmatrix} b_{vv} & b_{vh} \\ b_{hv} & b_{hh} \end{bmatrix}, \quad \mathbf{P} = \begin{bmatrix} p_{vv} & p_{vh} \\ p_{hv} & p_{hh} \end{bmatrix}, \quad (2)$$

$$\mathbf{R} = \begin{bmatrix} 1 & r_{vh} \\ r_{hv} & r_{hh} \end{bmatrix}, \quad \text{and} \quad \mathbf{T} = \begin{bmatrix} 1 & t_{vh} \\ t_{hv} & t_{hh} \end{bmatrix}. \quad (3)$$

Notice that \mathbf{R} and \mathbf{T} are relative matrices, meaning that the entire matrix has been divided by the first element which is then used as a common scalar constant. The phase factor $e^{j\phi}$ accounts for propagation to the target and back, and it depends on the exact position of the target phase center.

With some single antenna systems, the transmit and receive distortion matrices are simply the transpose of one another (i.e., the system is reciprocal) resulting in

the equation

$$\mathbf{M} = \mathbf{B} + e^{j\phi} a_{vv}^2 \mathbf{A}^T \mathbf{P} \mathbf{A}, \quad (4)$$

where the distortion matrix \mathbf{A} is given by

$$\mathbf{A} = \begin{bmatrix} 1 & a_{vh} \\ a_{hv} & a_{hh} \end{bmatrix}. \quad (5)$$

If the matrices \mathbf{B} , \mathbf{T} , and \mathbf{R} (or \mathbf{A} in the reciprocal case) can be determined, then the actual scattering matrix \mathbf{P} can be obtained from \mathbf{M} through one of the expressions

$$\mathbf{P} = e^{-j\phi} \frac{1}{r_{vv} t_{vv}} \mathbf{R}^{-1} (\mathbf{M} - \mathbf{B}) \mathbf{T}^{-1} \quad (6)$$

$$\mathbf{P} = e^{-j\phi} \frac{1}{a_{vv}^2} (\mathbf{A}^T)^{-1} (\mathbf{M} - \mathbf{B}) \mathbf{A}^{-1}, \quad (7)$$

which are obtained by rearranging equations (1) and (4). This representation assumes that the distortion matrices are invertible, which is generally true for actual radar systems. The propagation phase factor $e^{-j\phi}$ in equations (6) and (7) is difficult to measure, since the phase center of the target and the target position must be known exactly. However, in most cases only the relative phase of \mathbf{P} is desired.

By making a single measurement with no point target present, we can directly determine the matrix \mathbf{B} when the background is stationary ($\mathbf{M} = \mathbf{B}$ when $\mathbf{P} = 0$). Considering only a stationary background, the dual antenna and specialized single antenna problems in (1) and (4) are thus reduced to

$$\mathbf{N} = e^{j\phi} r_{vv} t_{vv} \mathbf{R} \mathbf{P} \mathbf{T} \quad (8)$$

$$\mathbf{N} = e^{j\phi} a_{vv}^2 \mathbf{A}^T \mathbf{P} \mathbf{A}, \quad (9)$$

where $\mathbf{N} = \mathbf{M} - \mathbf{B}$ is now a known matrix. If \mathbf{T} and \mathbf{R} (or \mathbf{A}) are known, the actual scattering matrix \mathbf{P} can be obtained from one of the expressions

$$\mathbf{P} = e^{-j\phi} \frac{1}{r_{vv} t_{vv}} \mathbf{R}^{-1} \mathbf{N} \mathbf{T}^{-1} \quad (10)$$

$$\mathbf{P} = e^{-j\phi} \frac{1}{a_{vv}^2} (\mathbf{A}^T)^{-1} \mathbf{N} \mathbf{A}^{-1}, \quad (11)$$

where we have simply replaced $\mathbf{M} - \mathbf{B}$ with \mathbf{N} in (6) and (7).

In the next two sections, techniques for determining the distortion matrices for the general dual antenna problem and the specialized single antenna problem are discussed. We will assume that the background scattering matrix has been removed as in equations (8)-(11) above.

3 General Dual Antenna System

Consider measurements of the form in (8) on three different targets with known scattering matrices. Using subscripts to denote the corresponding target and measurement scattering matrices, we obtain three matrix equations;

$$\mathbf{N}_i = e^{j\phi_i} r_{vv} t_{vv} \mathbf{R} \mathbf{P}_i \mathbf{T}, \quad \text{with } i = 1, 2, 3 \quad (12)$$

where \mathbf{N}_i and \mathbf{P}_i are known matrices, but \mathbf{R} and \mathbf{T} are unknown. Notice that a subscript is also used on the absolute phase to account for the positioning of the targets. The phase centers of the three targets will generally be located at different distances from the radar.

The following derivation requires that the target scattering matrix \mathbf{P}_i be invertible for at least one of the targets. Without loss of generality, we assume that this requirement is satisfied with the first target. Premultiplying both \mathbf{N}_2 and \mathbf{N}_3 by \mathbf{N}_1^{-1} and denoting the products as \mathbf{N}_T and $\bar{\mathbf{N}}_T$, we obtain the similarity transformations

$$\mathbf{N}_T = e^{j(\phi_2 - \phi_1)} \mathbf{T}^{-1} \mathbf{P}_T \mathbf{T} \quad (13)$$

$$\bar{\mathbf{N}}_T = e^{j(\phi_3 - \phi_1)} \mathbf{T}^{-1} \bar{\mathbf{P}}_T \mathbf{T}, \quad (14)$$

where $\mathbf{N}_T = \mathbf{N}_1^{-1} \mathbf{N}_2$, $\bar{\mathbf{N}}_T = \mathbf{N}_1^{-1} \mathbf{N}_3$, $\mathbf{P}_T = \mathbf{P}_1^{-1} \mathbf{P}_2$, and $\bar{\mathbf{P}}_T = \mathbf{P}_1^{-1} \mathbf{P}_3$.

We now consider an important property relating the eigenvalues and eigenvectors of similar matrices [15, pp. 165-166]. The eigenvalues and eigenvectors of the matrices \mathbf{N}_T and \mathbf{P}_T in equation (13) satisfy the relations

$$\mathbf{P}_T \mathbf{X}_T = \mathbf{X}_T \Lambda'_T \quad (15)$$

$$\mathbf{N}_T \mathbf{Y}_T = \mathbf{Y}_T \Lambda_T, \quad (16)$$

where Λ'_T and Λ_T are the diagonal matrices composed of the eigenvalues of \mathbf{P}_T and \mathbf{N}_T , respectively. The eigenvalue matrices are related by the expression

$$\Lambda'_T = \Lambda_T e^{j(\phi_1 - \phi_2)}. \quad (17)$$

Notice that the propagation phase difference, $\phi_1 - \phi_2$, between the phase centers of any two known targets can be determined using equation (17), even though this fact is not used in the present development. The corresponding eigenvectors of \mathbf{P}_T and \mathbf{N}_T form the columns of \mathbf{X}_T and \mathbf{Y}_T , respectively. Equations (15)-(17) state

that the eigenvalues of similar matrices are equal. Furthermore, the eigenvectors of \mathbf{P}_T and \mathbf{N}_T are related by the expression

$$\mathbf{Y}_T = \mathbf{T}^{-1}\mathbf{X}_T. \quad (18)$$

However, equation (18) does not uniquely specify \mathbf{T} since the eigenvectors comprising \mathbf{X}_T and \mathbf{Y}_T have arbitrary scale factors. Upon independently solving the eigenvalue problems in (15) and (16) for the matrices \mathbf{X}_T and \mathbf{Y}_T (arbitrarily choosing the scale factors), the matrix \mathbf{T} is uniquely specified by

$$\mathbf{Y}_T = \mathbf{T}^{-1}\mathbf{X}_T\mathbf{C} \quad \text{or} \quad (19)$$

$$\mathbf{T} = \mathbf{X}_T\mathbf{C}\mathbf{Y}_T^{-1}, \quad (20)$$

where \mathbf{C} is the diagonal matrix with elements $c_1 \neq 0$ and $c_2 \neq 0$ on the diagonal.

If the eigenvalues of \mathbf{P}_T are distinct, then the corresponding eigenvectors are linearly independent. Therefore, the matrix \mathbf{X}_T has rank two, which means that it is nonsingular and invertible [15, p. 149]. From equation (19), \mathbf{Y}_T is invertible if and only if \mathbf{X}_T is invertible. It is easily shown that distinct eigenvalues are obtained when

$$4\Delta(\mathbf{P}_T) \neq [\text{tr}(\mathbf{P}_T)]^2. \quad (21)$$

The notations $\Delta(\dots)$ and $\text{tr}(\dots)$ denote the determinant and the trace, respectively.

In the same way, the eigenvalues and eigenvectors of the matrices $\bar{\mathbf{N}}_T$ and $\bar{\mathbf{P}}_T$ in equation (14) satisfy the relations

$$\bar{\mathbf{P}}_T\bar{\mathbf{X}}_T = \bar{\mathbf{X}}_T\bar{\mathbf{\Lambda}}_T' \quad (22)$$

$$\bar{\mathbf{N}}_T \bar{\mathbf{Y}}_T = \bar{\mathbf{Y}}_T \bar{\mathbf{\Lambda}}_T, \quad (23)$$

where again $\bar{\mathbf{\Lambda}}_T'$ and $\bar{\mathbf{\Lambda}}_T$ are composed of the eigenvalues, and $\bar{\mathbf{X}}_T$ and $\bar{\mathbf{Y}}_T$ are the matrices whose columns are given by the corresponding eigenvectors. The eigenvalues of $\bar{\mathbf{P}}_T$ and $\bar{\mathbf{N}}_T$ are related by the expression

$$\bar{\mathbf{\Lambda}}_T' = \bar{\mathbf{\Lambda}}_T e^{j(\phi_1 - \phi_3)}. \quad (24)$$

From these results, we obtain another matrix equation for \mathbf{T} ;

$$\mathbf{T} = \bar{\mathbf{X}}_T \bar{\mathbf{C}} \bar{\mathbf{Y}}_T^{-1}, \quad (25)$$

where $\bar{\mathbf{C}}$ is the diagonal matrix with elements $\bar{c}_1 \neq 0$ and $\bar{c}_2 \neq 0$ on the diagonal.

Here, we have assumed that

$$4\Delta(\bar{\mathbf{P}}_T) \neq [\text{tr}(\bar{\mathbf{P}}_T)]^2. \quad (26)$$

Equating (20) and (25), we obtain

$$\mathbf{X}_T \mathbf{C} \mathbf{Y}_T^{-1} = \bar{\mathbf{X}}_T \bar{\mathbf{C}} \bar{\mathbf{Y}}_T^{-1}, \quad (27)$$

and after rearranging, (27) becomes

$$\mathbf{C} \mathbf{Y}_T^{-1} \bar{\mathbf{Y}}_T = \mathbf{X}_T^{-1} \bar{\mathbf{X}}_T \bar{\mathbf{C}}. \quad (28)$$

Expanding equation (28) and writing it in terms of four scalar equations, we have

$$c_1 \Delta(\mathbf{X}_T)(y_{22} \bar{y}_{11} - y_{12} \bar{y}_{21}) = \bar{c}_1 \Delta(\mathbf{Y}_T)(x_{22} \bar{x}_{11} - x_{12} \bar{x}_{21}) \quad (29)$$

$$c_1 \Delta(\mathbf{X}_T)(y_{22} \bar{y}_{12} - y_{12} \bar{y}_{22}) = \bar{c}_2 \Delta(\mathbf{Y}_T)(x_{22} \bar{x}_{12} - x_{12} \bar{x}_{22}) \quad (30)$$

$$c_2 \Delta(\mathbf{X}_T)(y_{11} \bar{y}_{21} - y_{21} \bar{y}_{11}) = \bar{c}_1 \Delta(\mathbf{Y}_T)(x_{11} \bar{x}_{21} - x_{21} \bar{x}_{11}) \quad (31)$$

$$c_2 \Delta(\mathbf{X}_T)(y_{11} \bar{y}_{22} - y_{21} \bar{y}_{12}) = \bar{c}_2 \Delta(\mathbf{Y}_T)(x_{11} \bar{x}_{22} - x_{21} \bar{x}_{12}), \quad (32)$$

where x_{mn} , y_{mn} , \bar{x}_{mn} , and \bar{y}_{mn} are the elements of the matrices \mathbf{X}_T , \mathbf{Y}_T , $\bar{\mathbf{X}}_T$, and $\bar{\mathbf{Y}}_T$, respectively. Assuming that equations (29)-(32) are all nonzero, we can obtain two expressions for c_2/c_1 and two for \bar{c}_2/\bar{c}_1 ;

$$\frac{c_2}{c_1} = \frac{(x_{11}\bar{x}_{21} - x_{21}\bar{x}_{11})(y_{22}\bar{y}_{11} - y_{12}\bar{y}_{21})}{(x_{22}\bar{x}_{11} - x_{12}\bar{x}_{21})(y_{11}\bar{y}_{21} - y_{21}\bar{y}_{11})} \quad (33)$$

$$\frac{c_2}{c_1} = \frac{(x_{11}\bar{x}_{22} - x_{21}\bar{x}_{12})(y_{22}\bar{y}_{12} - y_{12}\bar{y}_{22})}{(x_{22}\bar{x}_{12} - x_{12}\bar{x}_{22})(y_{11}\bar{y}_{22} - y_{21}\bar{y}_{12})} \quad (34)$$

$$\frac{\bar{c}_2}{\bar{c}_1} = \frac{(x_{22}\bar{x}_{11} - x_{12}\bar{x}_{21})(y_{22}\bar{y}_{12} - y_{12}\bar{y}_{22})}{(x_{22}\bar{x}_{12} - x_{12}\bar{x}_{22})(y_{22}\bar{y}_{11} - y_{12}\bar{y}_{21})} \quad (35)$$

$$\frac{\bar{c}_2}{\bar{c}_1} = \frac{(x_{11}\bar{x}_{21} - x_{21}\bar{x}_{11})(y_{11}\bar{y}_{22} - y_{21}\bar{y}_{12})}{(x_{11}\bar{x}_{22} - x_{21}\bar{x}_{12})(y_{11}\bar{y}_{21} - y_{21}\bar{y}_{11})} \quad (36)$$

If one equation is zero, then either (33) or (34) for c_2/c_1 and either (35) or (36) for \bar{c}_2/\bar{c}_1 will be indeterminate. However, the remaining expressions can be used to determine both c_2/c_1 and \bar{c}_2/\bar{c}_1 .

Based on the constraints in (21) and (26), we know that $\mathbf{X}_T^{-1}\bar{\mathbf{X}}_T$ is invertible and has a non-zero determinant. Hence, if two equations are zero, then they must be either the diagonal elements or the off diagonal elements of $\mathbf{X}_T^{-1}\bar{\mathbf{X}}_T$. In this situation, equations (33)-(36) are all indeterminate, and a solution for \mathbf{T} cannot be found. We must therefore require that

$$\bar{\mathbf{X}}_T \neq \mathbf{X}_T \boldsymbol{\alpha} \quad \text{and} \quad \bar{\mathbf{X}}_T \neq \mathbf{X}_T \boldsymbol{\beta}, \quad (37)$$

where

$$\boldsymbol{\alpha} = \begin{bmatrix} \alpha_1 & 0 \\ 0 & \alpha_2 \end{bmatrix} \quad \boldsymbol{\beta} = \begin{bmatrix} 0 & \beta_1 \\ \beta_2 & 0 \end{bmatrix}. \quad (38)$$

This constraint states that $\bar{\mathbf{P}}_T$ and \mathbf{P}_T can have no more than one common eigenvector.

The transmit distortion matrix \mathbf{T} can now be determined from either (20) or (25). Without loss of generality, we will show the result using (20). The first element of \mathbf{T} must be unity, and from (20) it is given by

$$\frac{1}{\Delta(\mathbf{Y}_T)} (c_1 x_{11} y_{22} - c_2 x_{12} y_{21}) = 1. \quad (39)$$

This expression can be used to obtain c_1 and c_2 in terms of the ratio c_2/c_1 ;

$$c_1 = \Delta(\mathbf{Y}_T) \left(x_{11} y_{22} - \frac{c_2}{c_1} x_{12} y_{21} \right)^{-1} \quad (40)$$

$$c_2 = \Delta(\mathbf{Y}_T) \left(\frac{c_1}{c_2} x_{11} y_{22} - x_{12} y_{21} \right)^{-1}. \quad (41)$$

The matrix \mathbf{R} can also be determined using a similar procedure. Postmultiplying both \mathbf{N}_2 and \mathbf{N}_3 by \mathbf{N}_1^{-1} , we obtain

$$\mathbf{N}_R = e^{j(\phi_2 - \phi_1)} \mathbf{R} \mathbf{P}_R \mathbf{R}^{-1} \quad (42)$$

$$\bar{\mathbf{N}}_R = e^{j(\phi_3 - \phi_1)} \mathbf{R} \bar{\mathbf{P}}_R \mathbf{R}^{-1}, \quad (43)$$

where $\mathbf{N}_R = \mathbf{N}_2 \mathbf{N}_1^{-1}$, $\bar{\mathbf{N}}_R = \mathbf{N}_3 \mathbf{N}_1^{-1}$, $\mathbf{P}_R = \mathbf{P}_2 \mathbf{P}_1^{-1}$, and $\bar{\mathbf{P}}_R = \mathbf{P}_3 \mathbf{P}_1^{-1}$.

Since equations (42) and (43) are again similarity transformations, we can uniquely specify \mathbf{R} by the relations

$$\mathbf{R} = \mathbf{X}_R \mathbf{D} \mathbf{Y}_R^{-1} \quad (44)$$

$$\mathbf{R} = \bar{\mathbf{X}}_R \bar{\mathbf{D}} \bar{\mathbf{Y}}_R^{-1}, \quad (45)$$

where the eigenvector matrices \mathbf{X}_R , \mathbf{Y}_R , $\bar{\mathbf{X}}_R$, and $\bar{\mathbf{Y}}_R$ satisfy the relations

$$\mathbf{N}_R \mathbf{X}_R = \mathbf{X}_R \mathbf{\Lambda}'_R \quad (46)$$

$$\mathbf{P}_R \mathbf{Y}_R = \mathbf{Y}_R \mathbf{\Lambda}_R \quad (47)$$

$$\bar{\mathbf{N}}_R \bar{\mathbf{X}}_R = \bar{\mathbf{X}}_R \bar{\mathbf{\Lambda}}_R' \quad (48)$$

$$\bar{\mathbf{P}}_R \bar{\mathbf{Y}}_R = \bar{\mathbf{Y}}_R \bar{\mathbf{\Lambda}}_R, \quad (49)$$

and the eigenvalue matrices are related by the expressions

$$\mathbf{\Lambda}'_R = \mathbf{\Lambda}_R e^{j(\phi_2 - \phi_1)} \quad (50)$$

$$\bar{\mathbf{\Lambda}}'_R = \bar{\mathbf{\Lambda}}_R e^{j(\phi_3 - \phi_1)}. \quad (51)$$

The matrices \mathbf{D} and $\bar{\mathbf{D}}$ are analogous to \mathbf{C} and $\bar{\mathbf{C}}$; they are diagonal with elements $(d_1 \neq 0, d_2 \neq 0)$ and $(\bar{d}_1 \neq 0, \bar{d}_2 \neq 0)$, respectively. Equations (44) and (45) are of the same form as (20) and (25), therefore equations (33)-(41) can be used to find expressions for d_1 and d_2 by replacing c with d and letting x_{mn} , y_{mn} , \bar{x}_{mn} , and \bar{y}_{mn} denote the elements of the matrices \mathbf{X}_R , \mathbf{Y}_R , $\bar{\mathbf{X}}_R$, and $\bar{\mathbf{Y}}_R$, respectively.

Since $\mathbf{P}_R = \mathbf{P}_T^T$ and $\bar{\mathbf{P}}_R = \bar{\mathbf{P}}_T^T$, the constraints on \mathbf{P}_T and $\bar{\mathbf{P}}_T$ are sufficient to guarantee a solution for \mathbf{R} as well as \mathbf{T} . The proof uses the relationship between the eigenvalues and eigenvectors of a matrix and its transpose [15, p. 164].

With the distortion matrices known, the absolute magnitude can be obtained by substituting back into one of the original measurements. Equating the elements of the matrices on both sides of (12) and taking the magnitude, we obtain for the mn^{th} element

$$|r_{vv} t_{vv}| = \frac{|(\mathbf{N}_i)_{mn}|}{|(\mathbf{R}\mathbf{P}_i\mathbf{T})_{mn}|}. \quad (52)$$

The best estimate of $|r_{vv} t_{vv}|$ will be obtained by choosing the target for which the theoretical matrix \mathbf{P}_i is most accurate.

Using (52), the scattering matrix \mathbf{P} for an unknown point target can be written in terms of the measured scattering matrix \mathbf{N} ;

$$\mathbf{P} = e^{-j\phi'} \frac{1}{|r_{vv}t_{vv}|} \mathbf{R}^{-1} \mathbf{N} \mathbf{T}^{-1}, \quad (53)$$

where ϕ' is the unknown absolute phase given by

$$\phi' = \phi + \tan^{-1} \left(\frac{\text{Im}\{r_{vv}t_{vv}\}}{\text{Re}\{r_{vv}t_{vv}\}} \right). \quad (54)$$

4 Specialized Single Antenna System

In general, single antenna radar systems, like dual antenna systems, have different distortion matrices for transmit and receive. Even though the single antenna affects the transmitted and received waves in a similar manner, the remaining portions of the transmit and receive paths through the system affect them differently. Therefore, equation (1) should be used to describe the measured scattering matrix for a general single antenna system, and the technique of Section 3 should be used in calibration.

In many cases, the antenna assembly is the major contributor to the distortion errors, and the contributions due to the different transmit and receive paths is negligible. Usually with such systems, care has been taken to make the transmit and receive paths practically identical, and only antenna effects need to be considered. The measured scattering matrix can then be described with equation (4), and a slightly different technique can be used in calibration. The major advantage of the technique is that only two known targets need to be measured to fully calibrate the measurement system. The technique is described in the following development.

Consider measurements of the form in (9) on two different targets with known scattering matrices. Using subscripted notation similar to that of equation (12), the measured scattering matrix of the i^{th} target is

$$\mathbf{N}_i = e^{j\phi_i} a_{uv}^2 \mathbf{A}^T \mathbf{P}_i \mathbf{A} \quad \text{with } i = 1, 2 \quad (55)$$

where \mathbf{P}_i is the known scattering matrix of the target. The unknown distortion matrix is \mathbf{A} . The calibration technique to be described requires a more restrictive condition on the form of the known scattering matrices than does the general technique of Section 3. With the present technique, both calibration targets must have invertible scattering matrices, whereas only one was required with the general technique.

Forming the products $\mathbf{N} = \mathbf{N}_2^{-1} \mathbf{N}_1$ and $\bar{\mathbf{N}} = (\mathbf{N}_2 \mathbf{N}_1^{-1})^T$, we obtain the two similarity transformations

$$\mathbf{N} = e^{j(\phi_1 - \phi_2)} \mathbf{A}^{-1} \mathbf{P} \mathbf{A} \quad (56)$$

$$\bar{\mathbf{N}} = e^{j(\phi_2 - \phi_1)} \mathbf{A}^{-1} \bar{\mathbf{P}} \mathbf{A}, \quad (57)$$

where $\mathbf{P} = \mathbf{P}_2^{-1} \mathbf{P}_1$ and $\bar{\mathbf{P}} = (\mathbf{P}_2 \mathbf{P}_1^{-1})^T$. This method can be applied to the specialized single antenna system only because the transmit and receive distortion matrices are related by a transpose. In a manner similar to that in Section 3, we can uniquely specify \mathbf{A} by the relations

$$\mathbf{A} = \mathbf{X} \mathbf{G} \mathbf{Y}^{-1} \quad (58)$$

$$\mathbf{A} = \bar{\mathbf{X}} \bar{\mathbf{G}} \bar{\mathbf{Y}}^{-1}, \quad (59)$$

where the matrices \mathbf{G} and $\overline{\mathbf{G}}$ are diagonal with elements ($g_1 \neq 0, g_2 \neq 0$) and ($\overline{g}_1 \neq 0, \overline{g}_2 \neq 0$), respectively. The eigenvector matrices \mathbf{X} , \mathbf{Y} , $\overline{\mathbf{X}}$, and $\overline{\mathbf{Y}}$ satisfy the expressions

$$\mathbf{P} \mathbf{X} = \mathbf{X} \Lambda' \quad (60)$$

$$\mathbf{N} \mathbf{Y} = \mathbf{Y} \Lambda \quad (61)$$

$$\overline{\mathbf{P}} \overline{\mathbf{X}} = \overline{\mathbf{X}} \overline{\Lambda}' \quad (62)$$

$$\overline{\mathbf{N}} \overline{\mathbf{Y}} = \overline{\mathbf{Y}} \overline{\Lambda}, \quad (63)$$

where the eigenvalue matrices Λ' , Λ , $\overline{\Lambda}'$, and $\overline{\Lambda}$ are related by

$$\Lambda' = \Lambda e^{j(\phi_1 - \phi_2)} \quad (64)$$

$$\overline{\Lambda}' = \overline{\Lambda} e^{j(\phi_2 - \phi_1)}. \quad (65)$$

Equating (58) and (59) and then rearranging, we obtain

$$\mathbf{G} \mathbf{Y}^{-1} \overline{\mathbf{Y}} = \mathbf{X}^{-1} \overline{\mathbf{X}} \overline{\mathbf{G}}. \quad (66)$$

Equation (66) is of the same form as (28), so g_1 and g_2 are given by equations (40) and (41) with g replacing c . Here, the elements x_{mn} , y_{mn} , \overline{x}_{mn} , and \overline{y}_{mn} denote the elements of the matrices \mathbf{X} , \mathbf{Y} , $\overline{\mathbf{X}}$, and $\overline{\mathbf{Y}}$, respectively. As in Section 3, we require the following constraints:

$$4\Delta(\mathbf{P}) \neq [\text{tr}(\mathbf{P})]^2 \quad (67)$$

$$4\Delta(\overline{\mathbf{P}}) \neq [\text{tr}(\overline{\mathbf{P}})]^2 \quad (68)$$

$$\overline{\mathbf{X}} \neq \mathbf{X}\alpha \quad \text{and} \quad \overline{\mathbf{X}} \neq \mathbf{X}\beta, \quad (69)$$

where α and β are of the form in equation (38).

By substituting equation (58) into (55) and equating the elements on both sides, we obtain for the mn^{th} element

$$|a_{vv}^2| = \frac{|(\mathbf{N}_i)_{mn}|}{|(\mathbf{A}^T \mathbf{P}_i \mathbf{A})_{mn}|}. \quad (70)$$

As in the general technique, the best estimate of $|a_{vv}^2|$ will be obtained by using the known target for which the theoretical matrix \mathbf{P}_i is most accurate.

We now have the effect of the distortion matrices determined to within an unknown phase factor. The scattering matrix for some unknown point target can be written as

$$\mathbf{P} = e^{-j\phi'} \frac{1}{|a_{vv}^2|} (\mathbf{A}^T)^{-1} \mathbf{N} \mathbf{A}^{-1}, \quad (71)$$

where ϕ' is the unknown absolute phase given by

$$\phi' = \phi + \tan^{-1} \left(\frac{\text{Im}\{a_{vv}^2\}}{\text{Re}\{a_{vv}^2\}} \right). \quad (72)$$

5 Application to Measuring the Propagation Characteristics of Random Media

Experimental investigations into the nature of propagation in random media have traditionally used two measurement configurations. The first type involves the use of a transmitter on one side of the random medium (considered as a layer) and a receiver on the other side. Measurements are made at a number of spatial locations through the layer to determine the statistics associated with the attenuation. In cases where only the extinction in the forward direction is desired, angular

resolution is obtained by making the antenna beamwidths small. This technique is cumbersome to use, particularly at oblique incidence to the random layer, due to the difficulty associated with proper pointing of the small beamwidth antennas. A second technique uses a transmitter and receiver placed at the same location (radar mode) on one side of the random layer and a point target on the other side. Because the received signal contains contributions from both the point target attenuated by the medium and the random layer itself, the precision associated with the measurement of the two-way attenuation depends upon the amplitude ratio of the two contributions [16, pp. 768-770]. Thus, the technique requires a point target with a large scattering cross section to obtain precise attenuation measurements. Furthermore, with this technique only the amplitude of the attenuation is measured; the propagation phase is usually ignored.

Recently, a polarimetric technique for measuring the propagation characteristics of random media was proposed and then demonstrated by measuring the characteristics of a forest canopy [17],[18]. The technique uses the same configuration as the second technique above, with the transmitter and receiver on one side of the random layer and a point target (trihedral) on the other side. The difference is that polarimetric measurements are made of the canopy scattering matrix with and without the presence of the trihedral underneath the canopy. The measurement without the trihedral yields the scattering matrix of the canopy alone, and the scattering matrix of the canopy/target combination is modeled as [17],[18]

$$\mathbf{S} = \mathbf{T} + e^{j\phi} l_{vv}^2 \mathbf{L}^T \mathbf{P} \mathbf{L}, \quad (73)$$

with

S = scattering matrix of the canopy/target combination

L = one-way relative propagation (loss) matrix of the canopy

P = scattering matrix of the point target alone

T = scattering matrix of the canopy (trees) alone.

The major restriction with the technique as described in [18] is that it assumes **L** to be a diagonal matrix. For the canopy and frequency (L-band) considered, this was a reasonable assumption to make. However, a more general technique without the restriction on the form of **L** would be applicable to a wider range of problems.

The calibration technique described in this paper can be used to extend the method above to cases where **L** is an arbitrary matrix. We notice that equation (73) is in the same form as (4) representing the specialized single antenna system. In essence, the propagation through the random medium is treated as a transformation analogous to that produced by the antenna for the single antenna system. By measuring the canopy alone and two additional known targets underneath the canopy, the method described in Section 4 can be used to determine the two-way extinction and the relative propagation (or loss) matrix **L** of the canopy.

The technique can be further extended by considering the propagation through the canopy as non-reciprocal. Denoting the loss matrices in the upward and downward directions through the canopy as **U** and **D**, respectively, the scattering matrix

of the canopy/target combination becomes

$$\mathbf{S} = \mathbf{T} + e^{j\phi} u_{vv} d_{vv} \mathbf{U} \mathbf{P} \mathbf{D}. \quad (74)$$

Since equation (74) is of the same form as (1), the method of Section 3 can be used to determine the two-way extinction and the relative loss matrices \mathbf{U} and \mathbf{D} .

The application of the techniques discussed in this paper to measuring the propagation characteristics of random media (specifically vegetation) will be the subject of future investigation by the authors.

6 Conclusions

A general polarimetric calibration technique has been developed, requiring the measurement of at most three known targets. The only constraints on the form of the scattering matrices for the known targets are given below.

- (1) At least one scattering matrix must be invertible (assume it is \mathbf{P}_1).
- (2) Both $\mathbf{P}_1^{-1}\mathbf{P}_2$ and $\mathbf{P}_1^{-1}\mathbf{P}_3$ must have distinct eigenvalues.
- (3) $\mathbf{P}_1^{-1}\mathbf{P}_2$ and $\mathbf{P}_1^{-1}\mathbf{P}_3$ must have no more than one common eigenvector.

The errors introduced by the transmitter and receiver are modeled by distortion matrices that alter the measured scattering matrix of the illuminated target. A set of eigenvalue problems are then solved on matrix products involving the measured and theoretical scattering matrices to determine the distortion matrices. Calibration of the absolute magnitude is achieved by inserting the measured distortion

matrices back into one measurement and solving for the magnitude. The two distinct advantages of the technique are that (1) almost any targets can be used and (2) no assumptions are made about the magnitude of the distortion.

A similar development has also been given for the reciprocal case, where the distortion matrix for receive is the transpose of that for transmit. Only two known targets are required to solve for the distortion matrix, assuming that the following constraints are satisfied.

- (1) Both scattering matrices \mathbf{P}_1 and \mathbf{P}_2 must be invertible.
- (2) Both $\mathbf{P}_2^{-1}\mathbf{P}_1$ and $(\mathbf{P}_2\mathbf{P}_1^{-1})^T$ must have distinct eigenvalues.
- (3) $\mathbf{P}_2^{-1}\mathbf{P}_1$ and $(\mathbf{P}_2\mathbf{P}_1^{-1})^T$ must have no more than one common eigenvector.

The technique is applicable to both laboratory and field measurements, with the known targets being chosen according to the application. For example, in a laboratory environment the emphasis should be placed on accuracy of the theoretical scattering matrices of the calibration targets. The sensitivity to positioning of the targets is only a secondary consideration, since one would conceivably have very fine control of target orientation. In field calibration, one should choose targets that are generally insensitive to positioning, since this aspect is the most difficult to control. The errors in the theoretical scattering matrices for these calibration targets can be determined with laboratory measurements using a different set of very accurate calibration targets. Hence, the actual scattering matrices can be determined.

Further research is being conducted to determine the best possible calibration targets to use with the techniques described in this paper. The results of this research and the implementation of the techniques will be considered in an additional paper to follow.

Acknowledgment

The authors would like to thank Mr. Paul Polatin for his constructive comments on the implementation of the calibration techniques given in this paper.

References

- [1] H. A. Zebker, J. J. van Zyl, and D. N. Held, "Imaging radar polarimetry from wave synthesis," *J. Geophys. Res.*, vol. 92, no. B1, pp. 683-701, Jan. 1987.
- [2] J. J. van Zyl, H. A. Zebker, and C. Elachi, "Imaging radar polarization signatures: Theory and observation," *Radio Sci.*, vol. 22, no. 4, pp. 529-543, July-Aug. 1987.
- [3] D. Guili, "Polarization diversity in radars," *Proc. IEEE*, vol. 74, no. 2, pp. 245-269, Feb. 1986.
- [4] A. Kozma, A. D. Nichols, R. F. Rawson, S. J. Shackman, C. W. Haney, and J. J. Shanne, "Multifrequency-polarimetric SAR for remote sensing," *Proceedings of IGARSS '86 Symposium, Zürich, ESA SP-254*, vol. I, pp. 715-719, Sept. 1986.
- [5] D. G. Goodenough and C. Livingstone, *IGARSS '85 Symposium Digest*, Amherst, MA, vol. II, p. 686, Oct. 1985.
- [6] F. T. Ulaby, T. F. Haddock, J. East, and M. W. Whitt, "A millimeter-wave network analyzer based scatterometer," *IEEE Trans. Geosci. and Remote Sensing*, vol. 26, no. 1, pp. 75-81, Jan. 1988.
- [7] M. W. Whitt and F. T. Ulaby, "Millimeter-wave polarimetric measurements of artificial and natural targets," *IEEE Trans. Geosci. Remote Sensing*, vol. 26, no. 5, pp. 562-573, Sept. 1988.

- [8] A. J. Blanchard and J. Rochier, "Bistatic radar cross section measurement facility," *Proceedings of IGARSS '87 Symposium*, Ann Arbor, MI, vol. I, pp. 545-548, May 1987.
- [9] R. M. Barnes, "Polarimetric calibration using in-scene reflectors," Rep. TT-65, MIT Lincoln Laboratory, Lexington, MA, Sept. 1986.
- [10] A. Freeman, C. Werner, and Yuhshen Shen, "Calibration of multipolarisation imaging radar," *Proceedings of IGARSS '88 Symposium*, Edinburgh, Scotland, vol. I, pp. 335-339, Sept. 1988.
- [11] S. Riegger, W. Wiesbeck, and A. J. Sieber, "On the origin of cross-polarization in remote sensing," *Proceedings of IGARSS '87 Symposium*, Ann Arbor, MI, vol. I, pp. 577-580, May 1987.
- [12] K. Sarabandi, F. T. Ulaby, and M. A. Tassoudji, "Calibration of polarimetric radar systems," Accepted for publication in *IEEE Trans. Geosci. Remote Sensing*, May 1989.
- [13] J. J. van Zyl, "Calibration of polarimetric images using only image parameters and trihedral corner reflector responses," Submitted for publication in *IEEE Trans. Geosci. Remote Sensing*, Jan. 1989.
- [14] F. T. Ulaby, P. Polatin, M. W. Whitt, and V. Liepa, "A general polarimetric calibration technique: theory and experiment, Part II - experiment", submitted for publication in *IEEE Trans. Geosci. Remote Sensing*, July 1989.

- [15] J. M. Gere and W. Weaver, Jr., *Matrix Algebra for Engineers*, Second Edition, Brooks/Cole Publishing Company, Monterey, CA, 1983.
- [16] F. T. Ulaby, R. K. Moore, and A. K. Fung, *Microwave Remote Sensing: Active and Passive, Vol. II - Radar Remote Sensing and Surface Scattering and Emission Theory*, Reading, MA: Addison Wesley, 1982.
- [17] F. T. Ulaby, M. W. Whitt, and M. C. Dobson, "Radar polarimetric observations of a tree canopy," *Proceedings of IGARSS '88 Symposium*, Edinburgh, Scotland, vol. II, pp. 1005-1008, Sep. 1988.
- [18] F. T. Ulaby, M. W. Whitt, and M. C. Dobson, "Measuring the propagation properties of a forest canopy using a polarimetric scatterometer," Accepted for publication in *IEEE Trans. on Antennas Propagat.*, 1989.

A GENERAL POLARIMETRIC RADAR CALIBRATION
TECHNIQUE: THEORY AND EXPERIMENT

PART II – EXPERIMENT

F.T. Ulaby

P. Polatin

M. Whitt

V. Liepa

July 31, 1989

Radiation Laboratory
Department of Electrical Engineering
and Computer Science
The University of Michigan
Ann Arbor, MI 48109-2122

Abstract

The accuracy achievable with the generalized calibration technique (GCT) introduced in the preceding paper is examined experimentally using an x-band radar system. The technique also is compared to the constrained calibration technique (CCT) and the isolated-antenna calibration technique (IACT). Measurements of the scattering matrices of test targets with known scattering properties reveal that the GCT, which is the most accurate of the three techniques, provides accuracies on the order of 0.3 dB in magnitude and 3° in phase and an effective polarization isolation of 50 dB.

1 INTRODUCTION

In the first [1] of this two-paper series, we introduced a generalized technique for calibrating a polarimetric radar system by measuring the distortion matrices of the transmit and receive antennas. We shall henceforth refer to it as the GCT, or *generalized calibration technique*. A similar calibration technique that also relies on measuring the distortion matrices of the antennas was proposed by Barnes [2] in 1986, except that it imposes some specific requirements on the forms of the scattering matrices of the targets used for calibration. Because of these constraints, we shall refer to this technique as the CCT, or *constrained calibration technique*. In this paper, we shall examine the calibration accuracy of these two techniques through experimental measurements conducted over the frequency range from 9-10 GHz. In addition, we shall also examine the calibration accuracy of a third technique that was proposed recently by Sarabandi et al. [3]. This third technique has the advantage that it is much simpler to apply than the other two techniques and it is insensitive to target orientation errors, but it is based on the major assumption that the radar antennas have perfect polarization isolation between their individual h- and v-ports. We shall refer to this technique as the IACT, or the *isolated-antenna calibration technique*.

The three calibration techniques will be evaluated using the same radar system and the same test targets. In each case, the radar will be calibrated and then used to measure the scattering matrix of a test target over the 9-10 GHz frequency range. The measured elements of the scattering matrix will then be compared to theoretically computed values.

2 MEASUREMENT SYSTEM

The scattering measurements reported in this paper were conducted in a 13-m long anechoic chamber using the setup diagrammed in Fig. 1. The radar uses an automatic vector

network analyzer (HP 8753) with a built-in frequency synthesizer. The HP 8753 unit is operated in a stepped-frequency chirp mode in 401 steps over the range from 1 to 2 GHz. The scatterometer unit shown in Fig. 1 includes an 8-GHz Gunn oscillator which mixes with the 1-2 GHz stepped- frequency signal to produce a 9-10 GHz stepped-frequency signal for transmission through the antenna. Upon reception of the backscattered signal, the signal frequency is down converted back to the 1-2 GHz (by mixing it with a sample signal from the 8-GHz Gunn oscillator) prior to returning the signal to the HP 8753 unit for processing.

Figure 2 is a block diagram of the scatterometer unit and the dual-polarized horn antenna. The orthomode transducer allows transmission and reception through a vertically polarized port and a horizontally polarized port, and the circulators and switches allow selection of any desired combination of transmit and receive polarization ports. The antenna is a pyramidal horn with a square aperture measuring 40.6 on each side, and its gain is 27.6 dB at 9.5 GHz. The overall system cross-polarization isolation is about 25 dB, which was determined by measuring the cross- polarized signals (hv and vh) backscattered from a metal sphere and comparing them to the levels of the like-polarized signals (vv and hh). By “overall system” we include cross-coupling between polarization channels due to not only the antennas, but the RF circuitry as well.

3 CALIBRATION TECHNIQUES

Even though we are using a single antenna for both transmission and reception, we should model the calibration problem in terms of the generalized schematic representation shown in Fig.3. Part (a) represents the condition when the polarization switch of the transmit antennas is energized to transmit a vertically polarized wave of amplitude E_0 . Because the antenna is non-ideal, the transmitted field E_t consists of a vertically polarized component ($t_{vv}E_0$) and a horizontally polarized component (t_{hv}/t_{vv}) E_0 ,

$$\mathbf{E}_t = t_{vv} E_0 \begin{bmatrix} 1 \\ t_{hv} \end{bmatrix} \quad (1)$$

where t_{hv} is a relative distortion element and represents the coupling between the v- and h-ports. The receive antenna is represented by two receivers, one measuring the “presumably” vertically polarized received signal E_r^v and the other measuring the “presumably” cross polarized received signal E_r^h . Each of these signals consists of two components, one of which accounts for the distortion properties of the receive antenna. For a point target with scattering matrix \mathbf{P} , the received electric field \mathbf{E}_r is given by

$$\mathbf{E}_r = \begin{bmatrix} E_r^v \\ E_r^h \end{bmatrix} = \frac{K}{r^2} e^{j\phi} r_{vv} t_{vv} \begin{bmatrix} 1 & r_{vh} \\ r_{hv} & r_{hh} \end{bmatrix} \begin{bmatrix} P_{vv} & P_{vh} \\ P_{hv} & P_{hh} \end{bmatrix} \begin{bmatrix} 1 \\ t_{hv} \end{bmatrix} \quad (2)$$

where

$$K = \left[\frac{P_t G_t G_r (\lambda)^2}{(4\pi)^2} \right]^{\frac{1}{2}}, \quad (3)$$

$P_t = E_0^2/2\eta$ is the transmitted power, G_t and G_r are the nominal gains of the transmit and receive antennas, ϕ is a phase factor that accounts for propagation to the target and back to the antenna, and r is the range to the point target.

Part (b) of Fig. 3 represents the condition when the polarization switch of the transmit antenna is energized to transmit horizontal polarization. This condition is given by the same expression (2) upon replacing the transmitted vector with

$$\mathbf{E}_t = t_{vv} E_0 \begin{bmatrix} t_{vh} \\ t_{hh} \end{bmatrix}, \quad (4)$$

and the two equations can be combined into the compact form

$$\begin{bmatrix} E_r^v \\ E_r^h \end{bmatrix} = \frac{K}{r^2} e^{j\phi} r_{vv} t_{vv} \mathbf{R} \mathbf{P} \mathbf{T} \begin{bmatrix} s_v \\ s_h \end{bmatrix} \quad (5)$$

with $(s_v, s_h) = (1, 0)$ when the polarization switch of the transmit antenna is energized to transmit vertical polarization and $(s_v, s_h) = (0, 1)$ when it is energized to transmit horizontal polarization.

If the radar is assumed to have distortionless antennas, which implies that $t_{ij} = r_{ij} = 0$ for $i \neq j$ and $t_{ij} = r_{ij} = 1$ for $i = j$, then the set of four measurements it makes will define a “measured” scattering matrix of the target, \mathbf{N} . With $\mathbf{R} = \mathbf{T} = \mathbf{I}$, the identity matrix, (5) becomes

$$\begin{bmatrix} E_r^v \\ E_r^h \end{bmatrix} = \frac{K}{r^2} \mathbf{N} \begin{bmatrix} s_v \\ s_h \end{bmatrix} \quad (6)$$

In the above expression, the phase reference is at the radar antenna. Upon equating (5) and (6), we obtain the result

$$\mathbf{N} = e^{j\phi} r_{vv} t_{vv} \mathbf{R} \mathbf{P} \mathbf{T} \quad , \quad (7)$$

which is the same as (8) of the previous paper [1]. Thus, \mathbf{N} is a directly measured quantity and the purpose of the calibration procedure is to determine the true scattering matrix of the target, \mathbf{P} .

3.1 Isolated Antenna Calibration Technique (IACT)

The IACT assumes that the coupling between polarization ports is sufficiently small to justify setting $t_{ij} = r_{ij} = 0$ for $i \neq j$, but allows t_{hh} to be different from t_{vv} and r_{hh} to be different from r_{vv} . In this case, (7) reduces to four simple equations

$$\begin{aligned}
n_{vv} &= e^{j\phi} r_{vv} t_{vv} P_{vv} , \\
n_{vh} &= e^{j\phi} r_{vv}^2 t_{vv} t_{hh} P_{vh} , \\
n_{hv} &= e^{j\phi} r_{vv} t_{vv}^2 r_{hh} P_{hv} , \\
n_{hh} &= e^{j\phi} r_{vv} t_{vv} r_{hh} t_{hh} P_{hh} .
\end{aligned} \tag{8}$$

According to the procedure given in Sarabandi et al. [3], the four complex quantities r_{vv} , r_{hh} , t_{vv} , and t_{hh} can be determined by conducting measurements against two targets, namely a conducting sphere and any other target that produces a cross-polarized signal. Moreover, it is not necessary to know the actual cross-section of the second target. The obvious advantage of this technique is that it is immune to orientation errors of the two calibration targets. Its disadvantage is that it does not account for cross-coupling between polarization ports.

3.2 Constrained Calibration Technique (CCT)

The CCT accounts for cross-coupling between polarization ports by attempting to measure all the elements of the distortion matrices, \mathbf{R} and \mathbf{T} , as well as the factor $r_{vv} t_{vv}$. To determine \mathbf{R} and \mathbf{T} , the procedure calls for measuring \mathbf{N} for each of three point targets characterized by the matrices [2]

$$\mathbf{P}_1 = P_0 \begin{bmatrix} 1 & 0 \\ 0 & 0 \end{bmatrix}, \quad \mathbf{P}_2 = P_0 \begin{bmatrix} 0 & 0 \\ 0 & 1 \end{bmatrix}, \quad \mathbf{P}_3 = P_0 \begin{bmatrix} 1 & 1 \\ 1 & 1 \end{bmatrix} . \tag{9}$$

A candidate target that would exhibit this behavior is an infinitesimally thin, conducting, circular, cylinder oriented vertically (\mathbf{P}_1), horizontally (\mathbf{P}_2), and at 45° (\mathbf{P}_3). In practice, if a cylinder is made very thin in order to approach the condition that it does not scatter an incident wave unless its electric field is parallel to the axis of the cylinder, the radar cross section of the cylinder becomes very small, which leads to inadequate signal to noise ratio, thereby reducing the accuracy of the measurement. Thus, a primary limitation of

the technique is that the constraints it places on the form of the scattering matrices of the calibration targets are very difficult to achieve in practice.

3.3 Generalized Calibration Technique (GCT)

The GCT introduced in the previous paper [1] also uses three calibration targets, but it does not require their matrices to have particular forms (except for being different). Both the CCT and GCT require that the matrices of the calibration targets be known, which means that their geometries should be such that we can compute their scattering matrices using exact (or fairly exact) theoretical expressions. Since at least one of the calibration target matrices should have non-zero cross-polarization elements, that calibration target cannot be an orientation-independent target (such as a sphere). Consequently, the CCT and GCT are inherently sensitive to errors associated with orientation of the calibration targets, in contrast with the IACT which is immune to orientation errors because it uses a sphere (of known radar cross section) and a second target whose radar cross section does not need to be known because it is not used in the calibration procedure.

A summary of the salient features of the three calibration techniques is provided in Table 1.

4 EXPERIMENTAL MEASUREMENTS

The radar system described in Section 2 was calibrated according to each of the three calibration techniques and then it was used to measure the scattering matrices of a 20-cm diameter conducting sphere and a 27-cm long vertical cylinder. Table 2 provides a summary of the calibration and test targets used.

The results for the conducting sphere are given in Fig. 4. Parts (a) and (b) show spectral plots of the like-Polarized scattering amplitudes, P_{vv} and P_{hh} ; each figure contains a plot of the scattering amplitude computed using the standard Mie solution and three plots based on the radar measurements. We observe that the GCT and IACT results

are within 0.1 dB of one another and within 0.3 dB of theory. The CCT results are higher than theory by about 3 dB for P_{vv} and lower by about 1 dB for P_{hh} . These large errors associated with the CCT are a result of assuming that the cylinders used for calibration satisfy the matrices given by (9) which state that $P_{hh} = 0$ for a vertical cylinder and $P_{vv} = 0$ for a horizontal cylinder. The cylinders used were all 30 cm in length and 0.234 cm in diameter. According to theoretical calculations for a vertically oriented cylinder with these dimensions [4], P_{hh} is about 30 dB lower than P_{vv} in the 9-10 GHz range. Thus, the results of Figs. 4(a) and 4(b) suggest that the difference between P_{vv} and P_{hh} should be much greater than 30 dB in order to reduce the error down to the levels attainable with the two other techniques.

Part (c) of Fig. 4 presents the “measured” spectrum of the cross-polarized scattering amplitude P_{vh} . According to theory, a conducting sphere does not depolarize; i.e., P_{vh} should be zero (or $-\infty$ on a dB scale). Hence, for a given calibration technique, the measured value of P_{vh} , relative to the value of P_{vv} (or P_{hh}), represents the effective polarization isolation provided by that technique. From the data in Figs. 4(a) and 4(c), the effective polarization isolation is found to be best for the GCT ($\simeq 50$ dB) and worst for the IACT ($\simeq 20$ dB). The CCT provides an effective isolation of $\simeq 30$ dB. According to Fig. 4(d), the measured phase of P_{hh} relative to that of P_{vv} , namely $(\phi_{hh} - \phi_v)$, is within 2° of theoretical for the GCT and IACT, but is off by more than 30° for the CCT.

Our second test target was a vertical cylinder, 27.1 cm long and 0.179 cm in diameter. The results for P_{vv} and P_{hh} (Figs. 5(a) and (b)) lead to the same conclusions stated earlier in connection with Figs. 4(a) and (b) for the sphere, namely that the GCT and IACT provide superior calibration accuracy than the CCT. Figure 5(c) presents the results for $(\phi_{hh} - \phi_{vv})$. We observe that the phase difference measured by the GCT and IACT are within about 3° of theoretical expectations, whereas the CCT is off by more than 30° .

5 CONCLUSIONS

According to the results of the experiments conducted to evaluate the calibration accuracies of the three calibration techniques examined in this paper, we offer the following conclusions:

1. Overall, the generalized calibration technique (GCT) provides the best accuracy and the constrained calibration technique (CCT) is the least accurate. The GCT can provide accuracies on the order of 0.3 dB in magnitude and 3° in phase and an effective polarization isolation of 50 dB.
2. Except when measuring targets whose cross-polarized scattering amplitudes (P_{vh} and P_{hv}) are much smaller than their like-polarized scattering amplitudes, the isolated-antenna calibration technique (IACT) provides results essentially identical with those observed for the GCT.

References

- [1] Whitt, M.W. and F.T. Ulaby, "A General Polarimetric Radar Calibration Technique: Theory and Experiment. Part I - Theory, submitted for publication in *IEEE Transactions on Geoscience and Remote Sensing*, July, 1989.
- [2] Barnes, R.M., "Polarimetric Calibration Using In-Scene Reflectors," Rep. TT-65, MIT Lincoln Laboratory, Lexington, MA, Sept. 1986.
- [3] Sarabandi, K., Ulaby, F.T., and Tassoudji, M.A., "Calibration of Polarimetric Radar Systems with Good Polarization Isolation," Submitted to *IEEE Transactions on Geoscience and Remote Sensing*, Dec. 1988.
- [4] Ruck, G.T., D.E. Barrick, W.D. Stuart, and C.K. Krichbaum, Radar Cross Section Handbook, Vol. 1, *Plenum Press*, New York, 1970.

Table 1: Salient features of the three techniques discussed in this paper for polarimetric calibration of a two-antenna polarimetric radar system.

Feature	GCT	CCT	IACT
Minimum Number of Calibration Targets	3	3	2
Types of Calibration Targets	Any 3 different targets with known scattering matrices	3 targets with specific scattering matrices (see Section 3.2)	conducting sphere, plus any depolarizing target
Accounts for Antenna Polarization Distortion	yes	yes	no
Sensitive to Orientation Error of Calibration Target	yes	yes	no

Table 2: Calibration and test targets used.

Targets	GCT	CCT	IACT
Cal Target 1	15-cm diameter metal sphere	vertical cylinder, $l=30\text{cm}$, $d=0.234\text{cm}$	15-cm diameter metal sphere $d=0.79\text{cm}$
Cal Target 2	45° cylinder, $l=27.1\text{cm}$, $d=0.79\text{cm}$	45° vertical cylinder $l=30\text{cm}$, $d=0.234\text{cm}$	45° cylinder, $l=27.1\text{cm}$, $d=0.79\text{cm}$
Cal Target 3	horizontal cylinder, $l=27.1\text{cm}$, $d=0.79\text{cm}$	horizontal cylinder, $l=30\text{cm}$, $d=0.234\text{cm}$	NONE
Test Target 1	20-cm diameter metal sphere	20-cm diameter metal sphere	20-cm diameter metal sphere
Test Target 2	vertical cylinder, $l=27.1\text{cm}$, $d=0.79\text{cm}$	vertical cylinder, $l=27.1\text{cm}$, $d=0.79\text{cm}$	vertical cylinder $l=27.1\text{cm}$, $d=0.79\text{cm}$

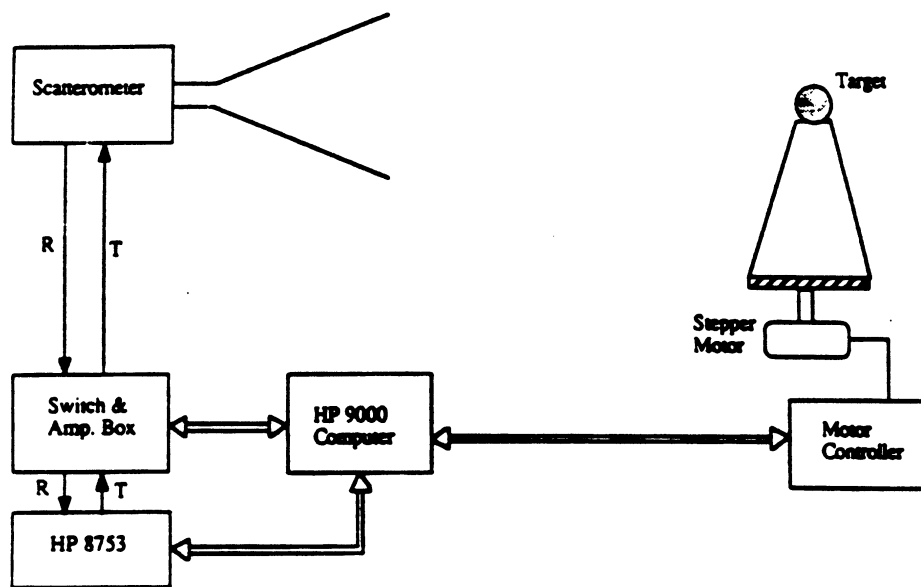


Figure 1. Automatic radar cross section measurement setup.

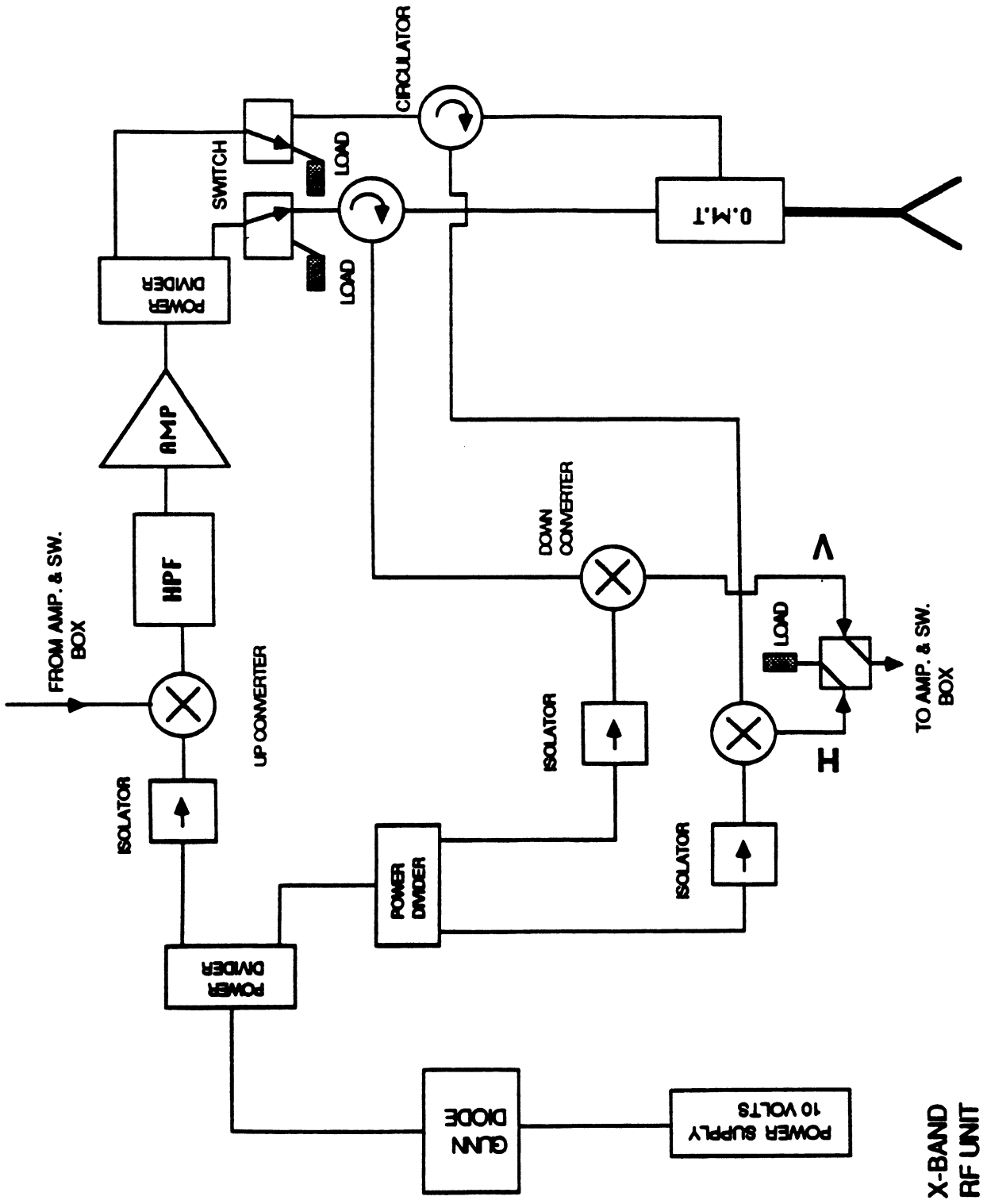


Figure 2. Block diagram of the X-band channel.

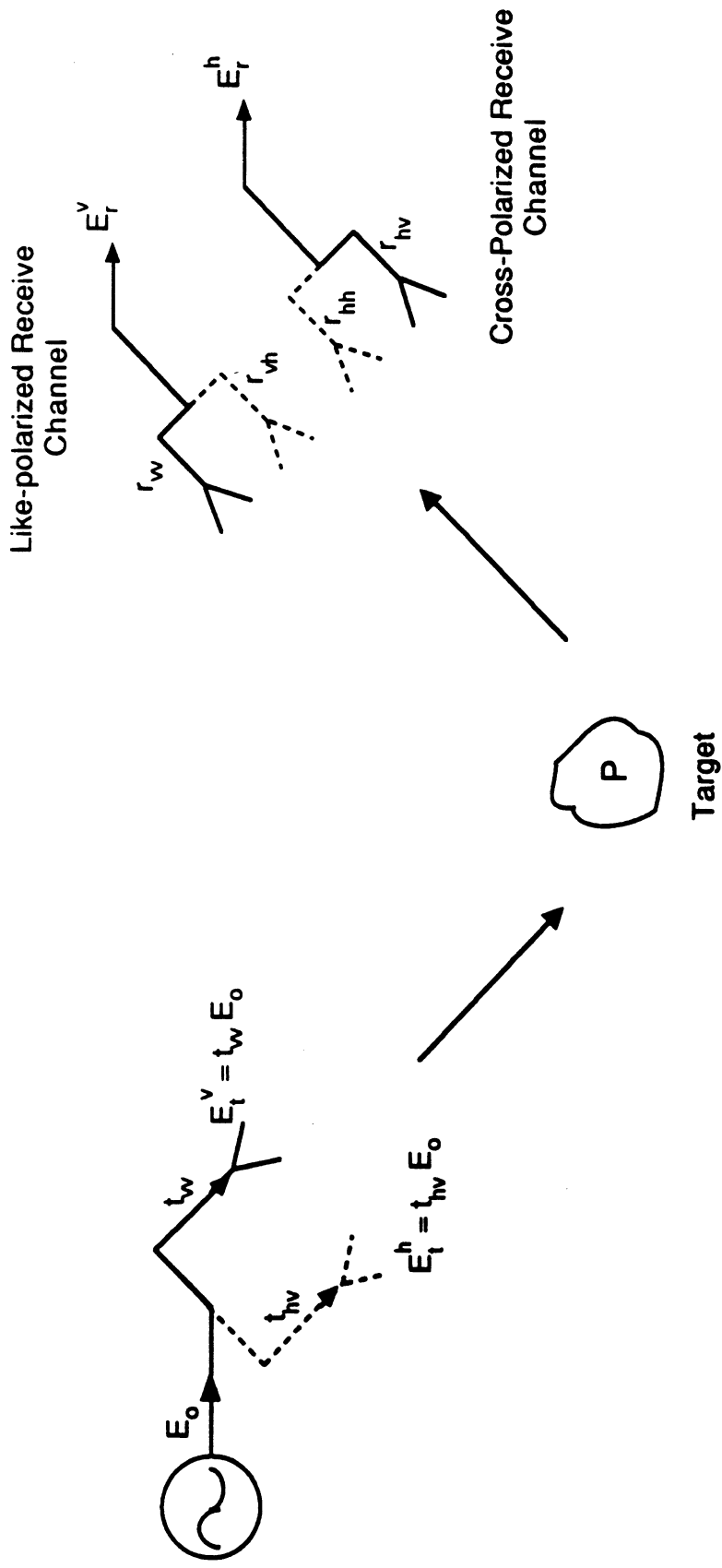
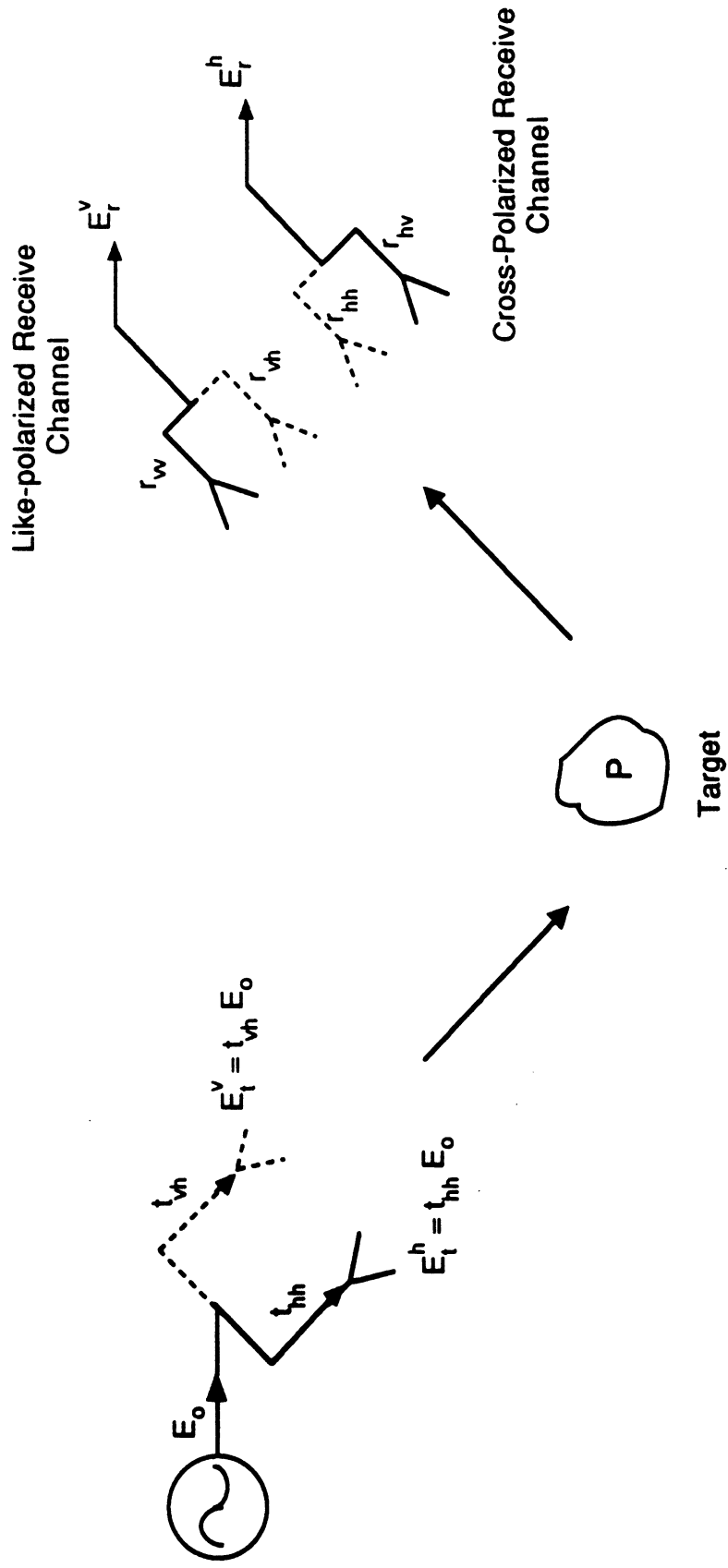
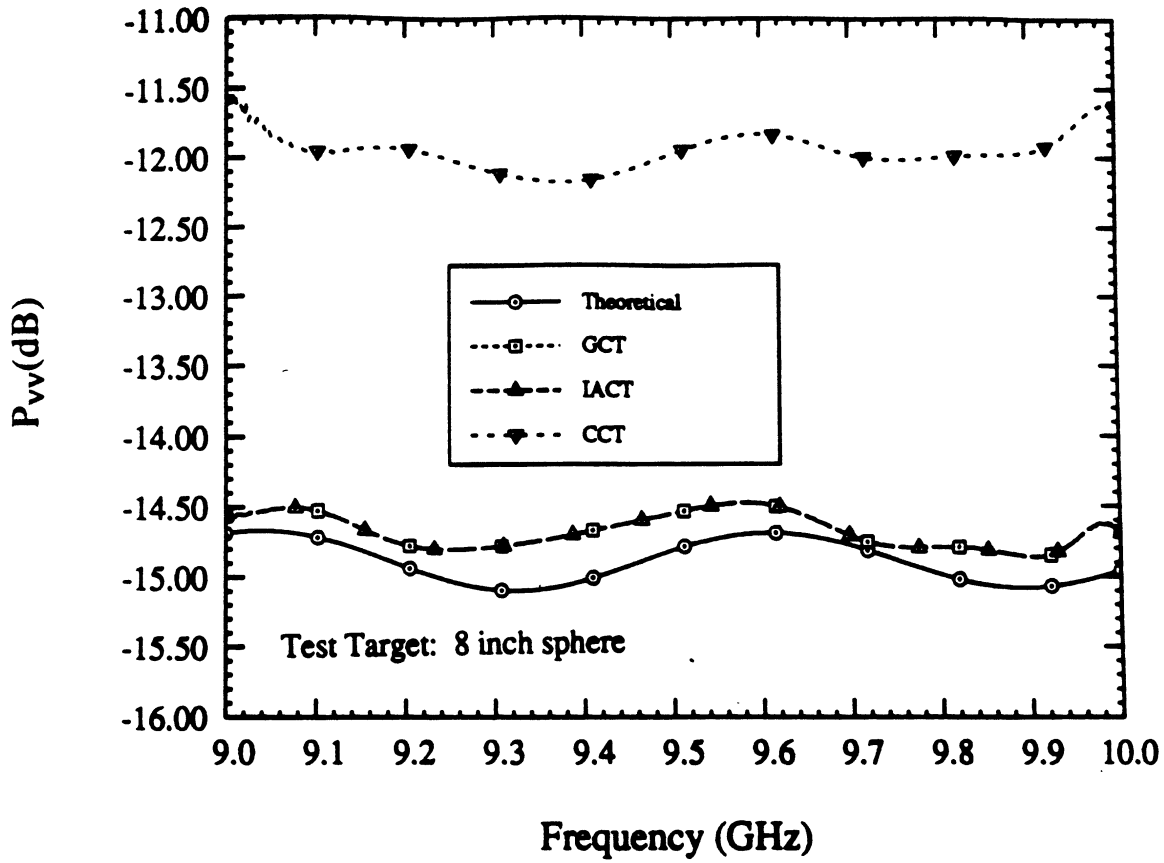


Figure 3. Schematic representation of transmit and receive antennas. The dashed lines represent polarization coupling. For an antenna with perfect polarization isolation, the coupling coefficients would be zero.

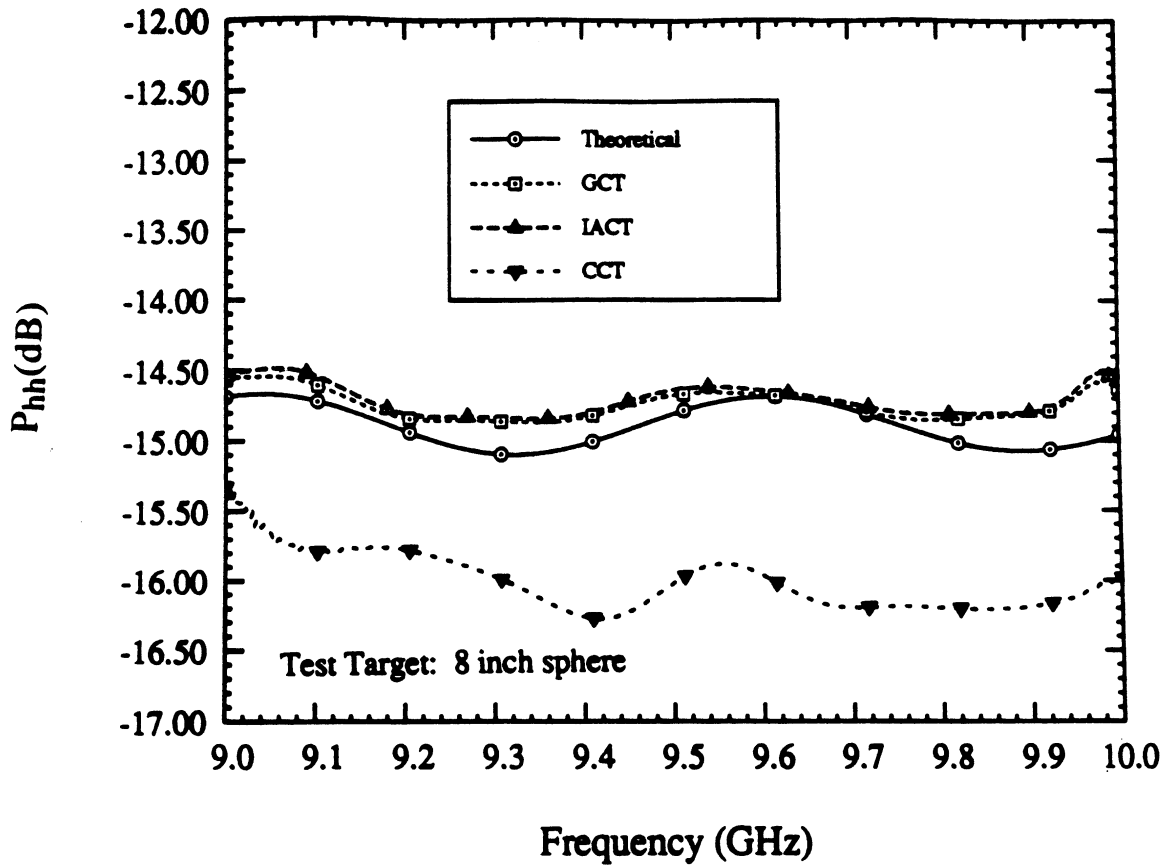


(b) h-polarized transmit configuration

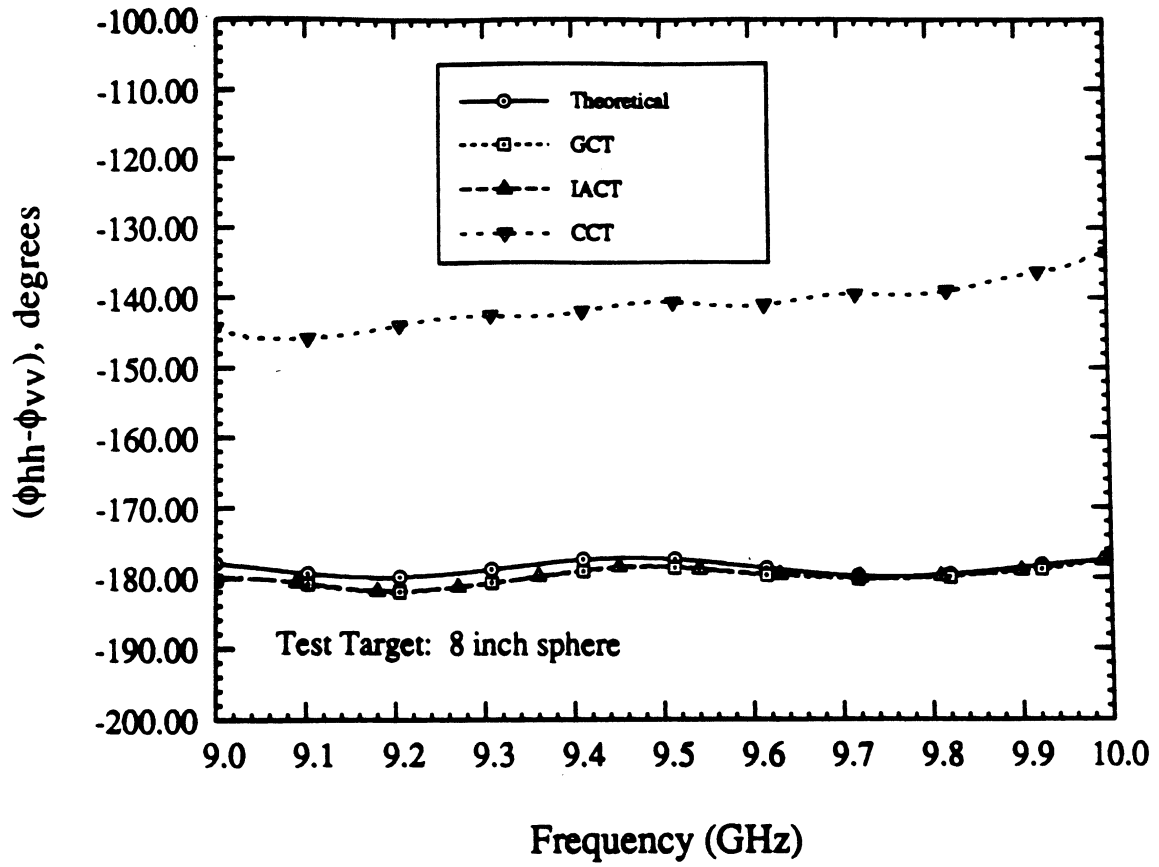


(a) P_{vv}

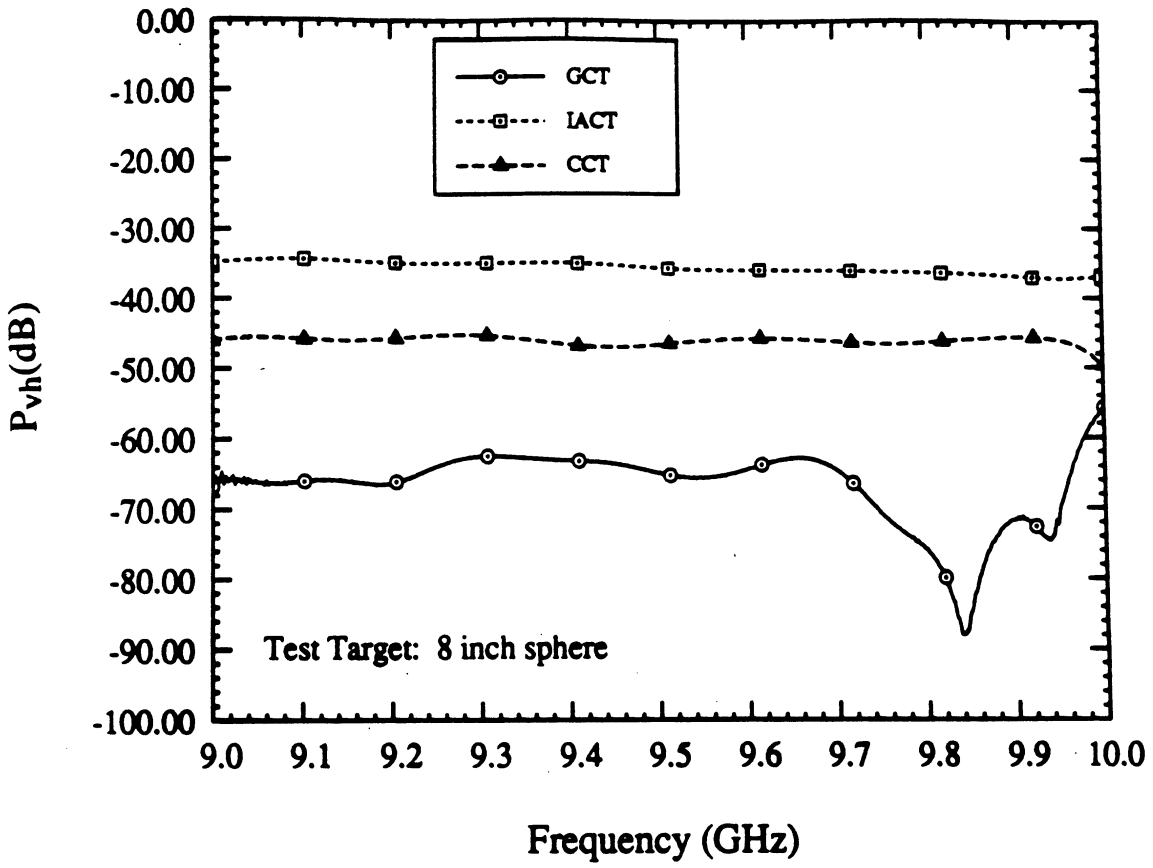
Figure 4. Plots of the theoretical and measured spectra for the 8-inch metal sphere.



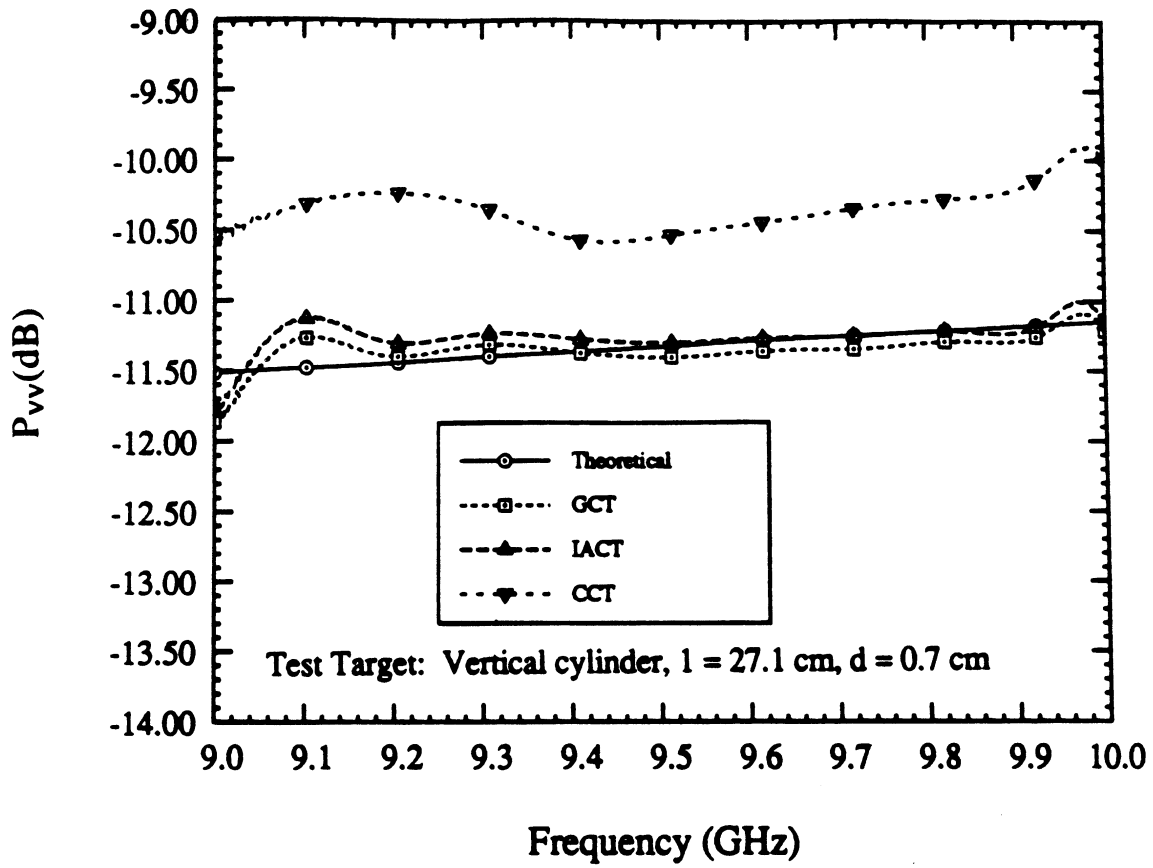
(b) P_{hh}



(d) $(\phi_{hh} - \phi_{vv})$

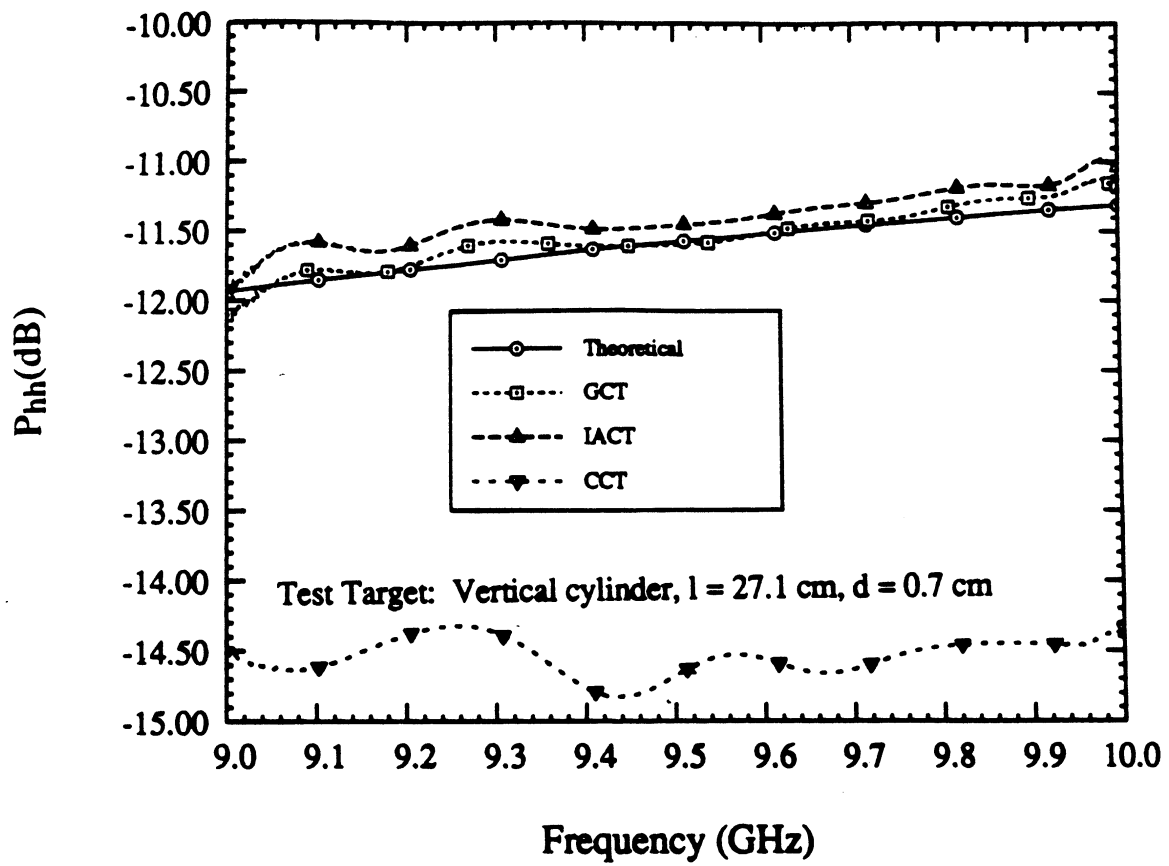


(c) P_{vh}

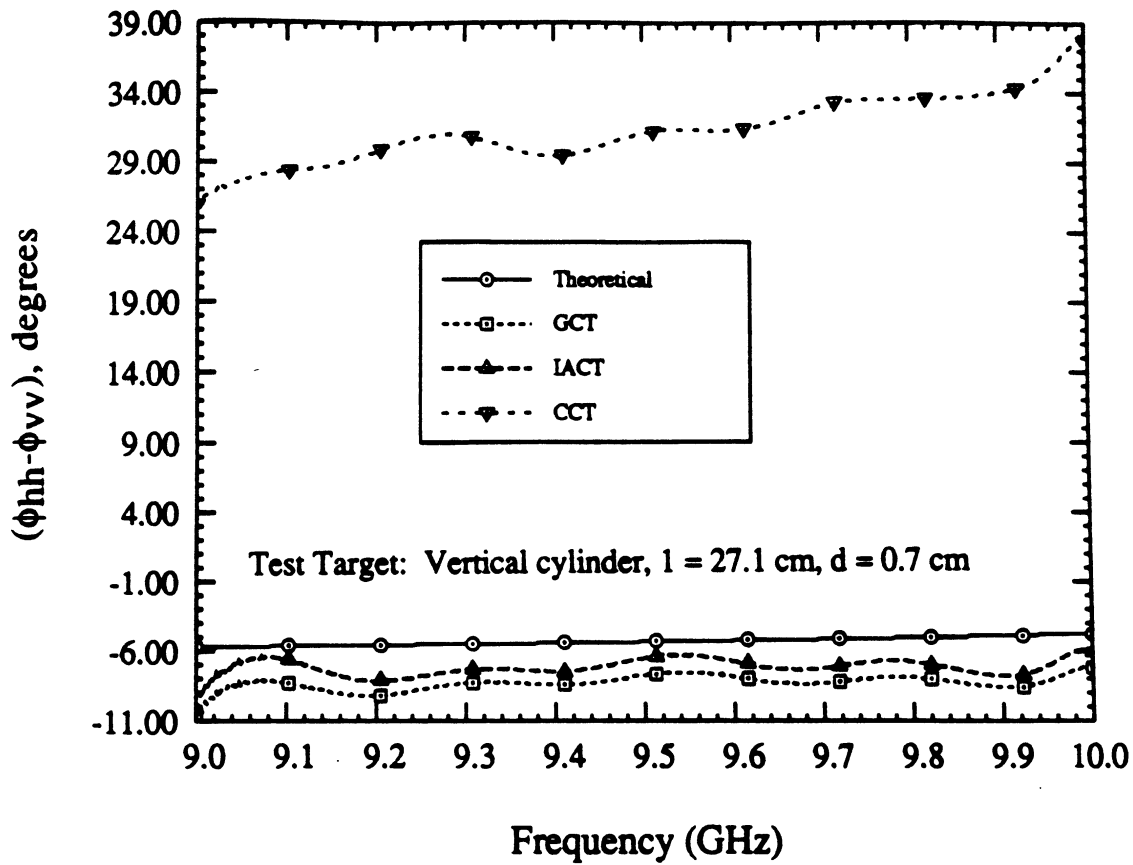


(a) P_w

Figure 5. Plots of the theoretical and measured spectra for the metal vertical cylinder.



(b) P_{hh}



(c) $\phi_{hh} - \phi_{vv}$

UNIVERSITY OF MICHIGAN



3 9015 03524 5102